Energy-Efficient Train Control with Onboard Energy Storage Systems considering Stochastic Regenerative Braking Energy

Wu, Chaoxian; Lu, Shaofeng; Tian, Zhongbei; Xue, Fei; Jiang, Lin

Energy-Efficient Train Control with Onboard Energy Storage Systems considering Stochastic Regenerative Braking Energy

Chaoxian Wu, Shaofeng Lu*, Zhongbei Tian, Fei Xue and Lin Jiang

***Abstract*—With the rapid development of energy storage technology, onboard energy storage systems(OESS) have been applied in modern railway systems to help reduce energy consumption. In addition, regenerative braking energy utilization is becoming increasingly important to avoid energy waste in the railway systems, undermining the sustainability of urban railway transportation. However, the intelligent energy management of the trains equipped with OESSs considering regenerative braking energy utilization is still rare in the field. This paper considers the stochastic characteristics of the regenerative braking power distributed in railway power networks. It concurrently optimizes the train trajectory with OESS and regenerative braking energy utilization. The expected regenerative braking power distribution can be obtained based on the Monte-Carlo simulation of the train timetable. Then, the integrated optimization using mixed integer linear programming (MILP) can be conducted and combined with the expected available regenerative braking energy. A generic four-station railway system powered by one traction substation is modeled and simulated for the study. The results show that by applying the proposed method, 68.8% of the expected regenerative braking energy in the environment will be further utilized. The expected amount of energy from the traction substation is reduced by 22.0% using the proposed train control method to recover more regenerative braking energy from improved energy interactions between trains and OESSs.**

***Index Terms*—Train trajectory, on-board energy storage system (OESS), regenerative braking energy, Monte-Carlo simulation, intelligent energy management**

NOMENCLATURE

Parameters

Δd_i	The i^{th} distance segments $[\mathrm{m}]$
η_o	Integrated energy conversion efficiency considering both motor efficiency and internal resistance of OESS
η_r	Transmission efficiency of the regenerative braking energy in the network
η_s	Integrated energy conversion efficiency considering both transmission loss and motor efficiency
$\overline{a}$	Preset maximum acceleration rate $[\mathrm{m/s^2}]$
$\overline{F_b}$	Maximum braking force of train motor $[\mathrm{kN}]$
$\overline{F_t}$	Maximum traction force of train motor $[\mathrm{kN}]$
$\overline{P_b}$	Maximum braking power of train motor $[\mathrm{kW}]$
$\overline{P_o}$	Maximum discharging/charging power of OESS $[\mathrm{kW}]$
$\overline{P_t}$	Maximum traction power of train motor $[\mathrm{kW}]$
ρ	Index of power supply sections of the studied railway system
θ_i	Gradient of Δd_i
$\tilde{P}_{reg,\rho}$	The expected available time-variant regenerative braking power distribution in power supply section ρ $[\mathrm{kW}]$
$\tilde{P}'_{reg,\rho}$	The expected available time-variant regenerative braking power distribution in power supply section ρ in piecewise form $[\mathrm{kW}]$
$\underline{a}$	Preset maximum deceleration rate $[\mathrm{m/s^2}]$
A	Davis coefficient $[\mathrm{kN}]$
B	Davis coefficient $[\mathrm{kN \cdot s/m}]$
b_x	coefficient of piecewise linear functions for expected regenerative braking power $[\mathrm{kW}]$
C	Davis coefficient $[\mathrm{kN \cdot s^2/m^2}]$
c_x	coefficient of piecewise linear functions for expected regenerative braking power $[\mathrm{kW/s}]$
E_{cap}	Capacity of OESS $[\mathrm{kJ}]$
g	Gravitational constant
i	Index of the distance segment
K	Number of piecewise section of the expected available regenerative braking power
k	Index of piecewise section of the expected regenerative braking power in the network from the perspective of the studied train
L	A sufficient large number
M_t	Mass of the train with OESS $[\mathrm{t}]$
N	The number of distance segments of the discretized track
SOC_1	Preset initial state of charge
T	Preset journey time $[\mathrm{s}]$
x	Index of the departure time instant of the studied train

Variables

This research project is supported and sponsored in part by the National Natural Science Foundation of China under Grant 52302380 and Grant 61603306, in part by the Funding by Science and Technology Projects in Guangzhou No. 2023A04J0312, in part by the National Science Foundation of Guangdong Province, China (Grant No.2023A1515012949), and in part by the Research Development Fund (RDF-18-01-04) of Xi'an Jiaotong-Liverpool University.

Chaoxian Wu is with the School of Systems Science and Engineering, Sun Yat-Sen University, Guangzhou, China (Email: wuchx35@mail.sysu.edu.cn)

Shaofeng Lu is with the Shien-Ming Wu School of Intelligent Engineering, South China University of Technology, China (Email: lushaofeng@scut.edu.cn)

Zhongbei Tian is with the School of Engineering, The University of Birmingham, UK (Email: z.tian@bham.ac.uk)

Fei Xue is with the Department of Electrical and Electronic Engineering, Xi'an Jiaotong-Liverpool University, China, 215123; (Email: Fei.Xue@xjtlu.edu.cn)

Lin Jiang is with the Department of Electrical Engineering and Electronics, The University of Liverpool, UK (Email: ljiang@liverpool.ac.uk)

*Corresponding Author: Dr. Shaofeng Lu, Shien-Ming Wu School of Intelligent Engineering, South China University of Technology, China. (Email: lushaofeng@scut.edu.cn),

α_x 0-1 variables to determine the time instant of the train in the network

$\alpha_{i,j}$ SOS2 variables to linearize energy utilization from the network in each Δd_i

$\beta_{i,j}$ SOS2 variables to linearize energy utilization from the network in each Δd_i

$\lambda_{i,1}$ 0-1 variables to determine the energy flow transmission in each Δd_i

$\lambda_{i,2}$ 0-1 variables to determine the energy flow transmission in each Δd_i

$\lambda_{i,3}$ 0-1 variables to determine the energy flow transmission in each Δd_i

$\mu_{i,j}^{\alpha}$ 0-1 variables to linearize energy utilization from the network in each Δd_i

$\mu_{i,j}^{\beta}$ 0-1 variables to linearize energy utilization from the network in each Δd_i

$\tilde{E}_{i,ch,reg}$ Expected energy received by OESS from the network in each Δd_i [kJ]

$\tilde{E}_{i,reg}$ Expected energy consumed by motor from the network in each Δd_i [kJ]

$E_{i,reg,o}$ Energy transmitted to other trains in each Δd_i [kJ]

$E_{i,res}$ Energy dissipated by resistors in each Δd_i [kJ]

$E_{i,s}$ Energy from substation in each Δd_i [kJ]

$E_{i,ch}^{k}$ Energy charged to OESS in each Δd_i [kJ]

$E_{i,dch}^{k}$ Energy discharged from OESS in each Δd_i [kJ]

$t'_{i,x}$ Auxiliary variables to determine the time instant of the train in the network [s]

v_i^2 Square of train speed when train reaches $\sum_1^{i-1} \Delta d_i$ [$\mathrm{m}^2/\mathrm{s}^2$]

$y_{i,1}$ Auxiliary variables to linearize energy utilization from the network in each Δd_i

$y_{i,2}$ Auxiliary variables to linearize energy utilization from the network in each Δd_i

I. Introduction

With the fast development of railway transportation worldwide, the energy consumption of the railway transportation systems is found to increase significantly [1], [2]. To reduce energy costs and meet the carbon-reduction targets of railway transportation, energy-saving technologies in railway systems continue to play a critical role. On the one hand, locating the optimal train control strategy and train scheduling to save energy is the most commonly used method since it does not need to change the infrastructure [1]. On the other hand, as one type of emerging technology, on-board energy storage systems (OESSs) have been utilized in modern railway transportation systems to absorb the regenerative braking energy and improve the energy efficiency further [3]–[5].

A. Energy-efficient Train Control Considering OESS

Energy-efficient Train Control (EETC), a classic problem in understanding how to operate the train from one station to another with a minimum energy cost within a given time, has been studied since the 1960s [6]. Many scholars have conducted pioneering work in this area using different methods from optimal control theories including but not limited to Pontryagin's Maximum Principle (PMP) [7]–[11], Dynamic Programming [12], [13], and different direct methods based on mathematical programming algorithms [14]–[18].

With the fast development of energy storage technology, more recent studies on EETC consider this emerging technology. Miyatake *et al.* [19], [20] investigate the optimal train trajectory with supercapacitor as OESS. In both papers, optimal train trajectories between two stations are found with the circuit model of supercapacitors by using sequential quadratic programming (SQP) and DP. Huang *et al.* [21] explore the energy-saving potential of supercapacitors by optimizing the train trajectory from the viewpoint of energy flow modeling for a single line by employing DP. Based on DP, for the battery-driven trains with continuous tractive effort, the optimal solution for train operation with Li-ion battery is also studied by Ghaviha *et al.* [22]. A general integrated optimization model for the train with a general model of OESS by applying mixed integer linear programming (MILP) is proposed by Wu *et al.* [23] with high energy-saving rate and computational efficiency. The work is extended in [24], and the management of OESS at stations and train trajectory are investigated, and it shows that appropriate charging/discharging management in inter-station journeys and dwellings is critical. Based on MILP, different dynamic power limits of supercapacitors, flywheels, and Li-ion batteries are also considered in [25] to optimize the train speed profiles with the three above types of OESSs, where the energy-saving potential comparisons among different types of energy storage as OESS are also given. Wu *et al.* [26] propose a two-step method based on convex programming (CP) to concurrently optimize the train speed, timetable, and OESS management based on the actual data from the Beijing metro system. An efficient heuristic algorithm is designed in [27] based on an improved artificial bee colony (ABC) algorithm to simultaneously obtain the optimal timetable and the matching capacity allocation scheme of OESSs.

On the one hand, combining EETC and OESSs has become an interesting research topic given the vast potential both technologies can offer in energy saving of railway transportation systems, and the analytical method [7]–[11], mathematical programming method [12], [13], [23], [25], [26], and heuristic method [27] are employed to find the optimal solution. On the other hand, researchers keep exploring the possible energy-saving benefits arising from cooperative operations between connected trains. The energy flowing inside the power network plays a crucial role in the net energy cost of the system due to the network's resistive costs and regenerative braking recuperation. As discussed below, well-designed cooperative train operations will realize further energy savings.

B. Cooperative Train Operations for Energy Saving

Making the most of the regenerative braking energy in railway systems by coordinating the trains in the network to save energy is widely studied by many researchers. In 2004, the train running time modification method for reducing power peaks and thus energy consumption was studied in [28]. Li *et al.* investigate the integrated optimization of the train trajectory and

timetable by maximizing the overlapping time for acceleration and braking events to make the most of the regenerative energy [29] by applying GA. In [30], train speed between switching points and each station's departure/arrival time is optimized for saving more net energy consumption based on CP and Kuhn–Tucker conditions. A mathematical energy consumption model of bidirectional trains running in the same power section based on train operation and electrical theories is proposed in [31], where GA is applied to generate an optimal speed profile for the second train to minimize energy consumption at the power substations. Taking into account the single-side feeding mode of the urban railways, Yang *et al.* employs GA to optimize the timetable of the Beijing Yizhuang line to fully utilize the regenerative braking energy [32], where the overlapping time for the accelerating and braking trains for single direction is maximized under the fixed train operation mode at each inter-station section. The model is further extended in [33], where the real-world train trajectories and both sides' feeding modes are considered in the model to maximize the energy interaction among trains for both directions. Taking the coasting points of each inter-station operation and station dwell times as variables, a multi-train traction power network modeling method by using a statistical approach with Monte-Carlo simulation is proposed to determine the system energy flow with regenerating braking trains in railway system [34]. A multi-train dynamical cooperation method was proposed without changing the timetable in [35]. The study shows that the regenerative braking energy can be calculated and then distributed to trains in the neighborhood by adjusting the train speed profiles. The paper conducted a perturbance analysis of the necessary condition under the precondition that the train runs in a long speed-holding journey. Based on DP and Simulated Annealing (SA) algorithm, Su *et al.* proposes a two-level model to jointly optimize the train timetable and driving strategy, in which the regenerative braking energy utilization significantly reduces the net mechanical energy consumption [36]. In [37], a real-time cooperative control method for train operation that can minimize the net energy consumption is proposed based on multi-agent reinforcement learning (MARL) algorithm, in which the driving strategy of each train can be real-time obtained according to the states of all trains. By taking the external power flow as an essential factor for Energy Efficient Train Control (EETC), the study [38] incorporates the spatial-temporal area into EETC. The spatial-temporal area combines the gradient information in space(distance) and the external power flow in time. Under the constraints of spatial-temporal area, the multi-train coordination problem was converted into the energy-efficient control of a train traveling in the spatial-temporal area. The problem was solved using PMP, and three arbitrary cases were shown to verify the effectiveness of the proposed method.

Based on the above discussion, it is clear that the connected trains will benefit from coordinated operations to realize the maximum energy-saving potential. Using different methods, successful case studies are reported in the literature, and some recent studies began to investigate how the external power flows will impose any impacts on EETC and energy saving [38]. And yet, few studies are dedicated to the effect of OESS and the dynamic spacial-temporal energy interaction inside the traction power network, leaving a challenging but essential research gap to fill. This paper aims to develop an agent-environment optimization framework in which OESS and statistical regenerative braking energy are modeled in detail to address this challenging problem discussed below.

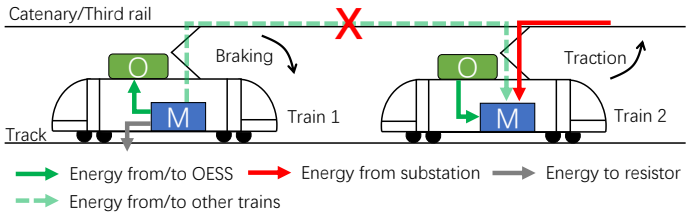

Fig. 1. The schematic of the energy flow for the metro train operation with OESS in the existing studies.

C. Problem Statement and Contributions

1) Problem statement: In the existing studies related to the train EETC with OESS, the regenerative braking energy that the OESSs cannot fully recover due to their limited power and capacity are all assumed to be dissipated by the resistors as heat. For instance, Figure 1 shows the energy flow between two trains with OESSs, Train 1 in braking mode and Train 2 in traction mode, in the practical railway system. The energy transmitted from OESS to the motor (green solid arrow), energy from the motor to OESS (green solid arrow), energy from the substation (red solid arrow), energy dissipated by braking resistor (gray solid arrow), and energy from Train 1 to Train 2 (green dashed arrow) can be found. In the figure, the "cross" shows that the energy from Train 1 to Train 2 is not considered in the previous relevant studies [23], [25]. This assumption compulsorily shuts off the connection of each train. It ignores the possibility of the energy exchange among trains with OESSs in the network, which is impractical in real applications.

Whether the OESSs are fully charged or not, if the regenerative braking energy can be stored in OESS and utilized by other trains concurrently during the operation, the energy consumption of the entire system can be reduced even further. It is noted that through proper coordination of train operations in the line, the regenerative braking energy can be further utilized to improve the energy efficiency of the railway system. Nevertheless, due to the ignorance of the possible energy exchange among trains with OESSs, their mutual coordination is still not discussed in the field of study. In addition, in the existing studies related to the coordination of the trains to save energy, the components involved are typically only trains and substations, and energy storage has not been considered for further coordination, not to mention the complex spatial-temporal energy dynamics in the traction power networks.

2) Contributions: To tackle the operation optimization problem of metro systems with OESS, this paper proposes an optimization framework to optimize the train trajectory to further utilize the OESS as well as the regenerative braking energy in the systems at the planning stage, and it is a significant extension of [23] which only deals with the optimization on the train with

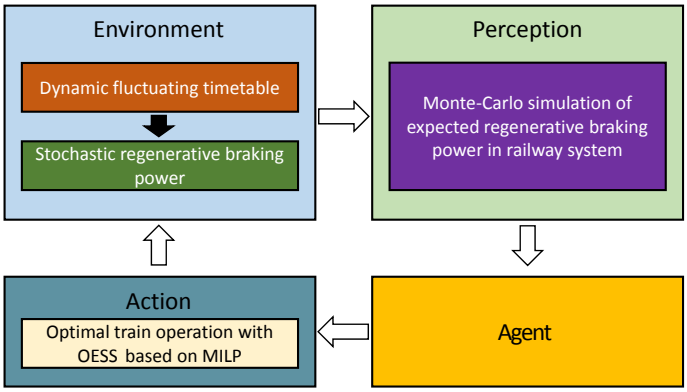

Fig. 2. An agent-environment structure of the train and railway power network. The train is the intelligent "agent" to perceive the environment using Monte-Carlo simulation to obtain the information of stochastic regenerative braking power and take optimal action to minimize the long-term expected energy cost via actuation to offer an impact on the environment.

OESS not considering the energy interaction with other trains in the network. In this paper, the stochastic characteristic of the railway network is brought by the running time variation of the train services in the network, which leads to the stochastic value and distribution of the traction/regenerative braking power in the environment. As shown in Figure 2, an agent-environment framework illustrates the relationship between trains and the environment. In this structure, the Monte-Carlo simulation as the "perception" method is first applied to generate the expected regenerative braking power that the OESSs cannot absorb from the viewpoint of long-term operation. This expectation is regarded as the environment to be perceived by every train running in the network. Then, based on the simulation results, an integrated mixed integer linear programming (MILP) model is proposed to optimize the train trajectory with OESS to minimize the net energy consumption by considering the stochastic regenerative braking energy in the environment. It should be noted that this metro-related method is not feasible and practical in rail systems like high-speed rail, diesel trains, trams, etc., with different system structures and application scopes.

In summary, the main contributions of this paper are listed as follows:

- Different from the existing research considering only the single train and OESS [19], [20], [23], [25], [39], this paper proposes a novel optimization framework to obtain the optimal train trajectory with OESS considering the utilization of regenerative braking energy. The optimal catenary/third rail power, OESS power, and utilized regenerative braking power are concurrently optimized to minimize the net energy consumption and maximize the expected utilization of the available regenerative braking energy. The case study also shows that the OESS can improve the energy efficiency of the entire system when the regenerative braking energy from other trains can be stored and utilized afterward.
- Different from the existing methods with deterministic information of environment and putting multiple/all trains in one optimization process with significant problem size, e.g., [33], [35]–[38], this paper adopts an agent-environment framework to achieve the long-term optimal solutions for each train service with consideration of the spacial-temporal influence of other trains in the network. The proposed model has a smaller problem size, enabling an efficient solution for achieving optimal coordination of multiple/all trains in the network to reduce energy consumption.

The remainder of the paper is organized as follows: Section II discusses the EETC considering OESSs and the modeling of the expected regenerative braking power. Section III presents a numerical experiment using a generic railway system to show the effectiveness and energy-saving performance of the proposed method. Section IV concludes the research findings. In the Appendix section, we illustrated the detailed modeling procedure for stochastic braking energy in the environment.

II. EETC Model Considering OESSs and External Energy Information in Environment

This section gives the detailed procedure to optimize the train trajectory with OESS considering external energy information in environment. The external energy information in environment is obtained by following the simulation process proposed in Appendix with the first step shown in Appendix.A to simulate the stochastic train running time, and the second step presented in Appendix.B to extract the expected regenerative braking power $\tilde{P}_{reg,\rho}$ in the environment. $\tilde{P}_{reg,\rho}$ is then input in the proposed EETC model as the external energy information in modelling and optimization process.

A. Kinematics of the Single-Train Movement

Similar to the model proposed in [23], the track length D between two adjacent stations is divided into N segments, as the Δd_i shown in Figure 3. As a result, there are $N+1$ speed points v_i in total. In the model, the train is assumed to do uniformly accelerated/decelerated motion in each Δd_i. As a result, the acceleration/deceleration a_i in Δd_i can be expressed by (1).

$$a_i = \pm \frac{v_{i+1}^2 - v_i^2}{2\Delta d_i} \tag{1}$$

Here, the positive value of a_i implies the acceleration, and the negative value implies a deceleration operation.

To ensure the riding comfort of the passengers and the operational limit of the train vehicle, the acceleration/deceleration should be limited by the maximum allowed value $\underline{a}$ and $\overline{a}$, as shown in (2).

$$-\underline{a} \leq a_i \leq \overline{a} \tag{2}$$

The relevant constraints need to be added to guarantee the proposed model's feasibility. First, the initial speed v_1 and terminal speed v_{N+1} need to be preset as in (3).

$$v_1^2 = 0, \quad v_{N+1}^2 = 0 \tag{3}$$

The relationships among the speed-related variables, v_i, v_i^2, $v_{i,ave}^2$ and $\frac{1}{v_{i,ave}}$, are not linear. These relationships can be linearized using the proposed method discussed in [23].

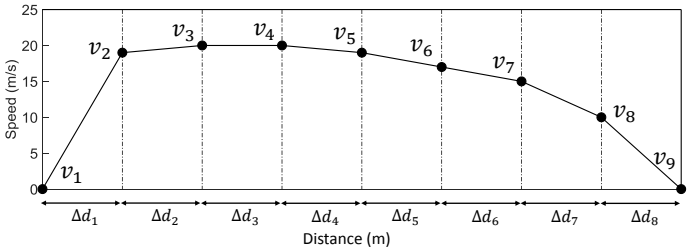

Fig. 3. An example of the discretization of the track length in the proposed method. The number of Δd_i, denoted by N, is 8, and nine determinant speed points are denoted by v_i, i=1,2,...,9.

For each Δd_i, the average speed $v_{i,ave}$ can be calculated using (4).

$$v_{i,ave} = \frac{v_i + v_{i+1}}{2} \tag{4}$$

Thus, the elapsed time Δt_i for each Δd_i is shown in (5).

$$\Delta t_i = \frac{\Delta d_i}{v_{i,ave}} \tag{5}$$

To guarantee the punctuality and operational requirement, the constraint of total journey time T should be added, as shown in (6).

$$\sum_{i=1}^{N} \Delta t_i = T \tag{6}$$

B. Consideration of the Expected Regenerative Braking Power

As shown in Figure 4-(a), the black solid line is the expected available time-variant regenerative braking power distribution in power supply section ρ, and it can be expressed with the function shown in (7).

$$\tilde{P}_{reg,\rho} = f(t) \tag{7}$$

where t is the time instant.

It needs to be clarified that $\tilde{P}_{reg,\rho}$ is formed by the trains following simulated timetables (referred to as the "sampled trains" below). To integrate $\tilde{P}_{reg,\rho}$ with the proposed single-train model above, the available regenerative braking energy that can be utilized by single-train operation needs to be extracted. The gray square in Figure 4-(a) represents the running time of a specific inter-station train service to be optimized (Referred to as the "studied train" below). In this running time horizon, the expected generated and consumed regenerative braking energy by sample trains serving the same inter-station section for same service cycle as the studied train need to be deducted from/compensated back to the $\tilde{P}_{reg,\rho}$ as these sampled trains are not supposed to directly contribute to the environment from the viewpoint of the studied train and their impacts need to be off-set by the deduction or compensation procedure as demonstrated by Figure 4-(b).

As shown in Figure 4-(b), $\tilde{P}_{reg,\rho}$ excludes the expected used regenerative braking power by the sampled trains; thus, this part needs to be compensated to the environment since the studied train can still use it, shown as the orange area in Figure 4-(b). In addition, $\tilde{P}_{reg,\rho}$ also contains the expected regenerative braking power from the sampled trains. This part should be eliminated since the studied train cannot use it, as the gray area shown in Figure 4-(b). After the recalculation procedure of the expected regenerative braking power distribution in the environment from the viewpoint of the studied train, $\tilde{P}'_{reg,\rho}$ can be obtained. Then the piecewise linear approximation is introduced, shown as the red dashed lines in the figure, to approximate $\tilde{P}'_{reg,\rho}$. Assuming that there are K piecewise linear sections for the approximation, it can be represented by using (8).

$$\tilde{P}'_{reg,\rho} \approx \begin{cases} f'_1(t) = c_1 t + b_1, & \text{for} \quad t_0 \le t \le t_1 \\ f'_2(t) = c_2 t + b_2, & \text{for} \quad t_1 \le t \le t_2 \\ \vdots & \\ f'_x(t) = c_x t + b_x, & \text{for} \quad t_{x-1} \le t \le t_x \\ \vdots & \\ f'_K(t) = c_K t + b_K, & \text{for} \quad t_{K-1} \le t \le t_K \end{cases} \tag{8}$$

where t_0, t_1, t_2, ... , t_x, ... , t_K are the time instant for the piecewise linear sections, f'_1, f'_2, ... , f'_x, ... , f'_K are the approximated linear functions, c_1, c_2, ... c_x, ... , c_K and b_1, b_2, ... b_x, ... , b_K are the coefficient for the piecewise functions.

As the approximation of the expected regenerative braking power is obtained, it can be utilized by adjusting the train operation. The expected regenerative braking power the train can utilize in each Δd_i depends on the corresponding time instant. Due to the discretization of the proposed model, the time instant, denoted as t'_i, of the train from departure to any Δd_i can be calculated using (9).

$$t'_i = t_x + \sum_{1}^{i-1} \Delta t_i + \frac{1}{2}\Delta t_i \tag{9}$$

Here, the $\frac{1}{2}\Delta t_i$ is the midpoint of the elapsed time of each Δd_i that is used to approximate the time instant together with the accumulated value of the previous journey. It can be observed that this approximation is more accurate with the shorter Δd_i.

C. Energy Flow during Movement

The kinetic energy change of the train $E_{i,v}$ in each Δd_i can be expressed in (10).

$$E_{i,v} = \frac{1}{2} M_t (v_{i+1}^2 - v_i^2) \tag{10}$$

where M_t is the total mass of the train with OESS.

When the train is running on the track, it is imposed with drag force $F_{i,drag}$ in each Δd_i estimated by the Davis Equation based on Davis coefficient A, B and C shown in (11).

$$F_{i,drag} = A + B v_{i,ave} + C v_{i,ave}^2 \tag{11}$$

As a result, the work of the drag force $E_{i,f}$ can be obtained in each Δd_i as shown in (12).

$$E_{i,f} = F_{i,drag} \Delta d_i \tag{12}$$

In addition, since there are varied gradients along the track, the work of the gravity $E_{i,p}$, which is also the potential change

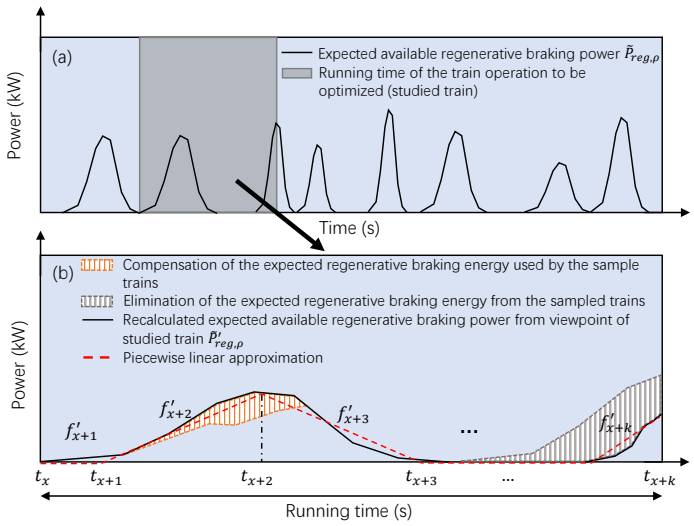

Fig. 4. (a) The obtained expected time-variant available regenerative braking power in the environment formed by the sampled trains; (b) The piecewise linear approximation of the recalculated expected available regenerative braking power from the viewpoint of the studied train by compensating and eliminating the expected regenerative braking power affected by the sampled trains.

of the train caused by gravity, is applied to the train. Thus, each Δd_i can be obtained as shown in (13).

$$E_{i,p} = M_t g \Delta d_i \theta_i \tag{13}$$

where a positive value of θ_i represents the down-slope, and a negative one represents the up-slope.

During the journey, the train can consume the energy from the traction substation $E_{i,s}$, the energy discharged by the OESS $E_{i,dch}$ and the expected regenerative braking energy from other trains $\tilde{E}_{i,reg}$ when the train is motoring. Here, the work of the train motor, denoted as $E^+_{i,m}$, can be expressed in (14).

$$E^+_{i,m} = E_{i,s}\eta_s + E_{i,dch}\eta_o + \tilde{E}_{i,reg}\eta_r \tag{14}$$

where η_s, η_o, and η_r are the energy supply sources' energy conversion efficiency, respectively.

When the train is braking, the motor is in regenerative braking mode, and part of the energy can be delivered to the OESS, denoted as $E_{i,ch}$ here. Part of the energy will be transmitted to other trains through catenary/third rail, denoted as $E_{i,reg,o}$, and the rest of the energy will be dissipated by resistors, denoted as $E_{i,res}$. Thus, during the braking mode, the work of the train motor, denoted as $E^-_{i,m}$, is represented in (15).

$$E^-_{i,m} = -\frac{E_{i,ch}}{\eta_o} - E_{i,reg,o} - E_{i,res} \tag{15}$$

Here the state of charge (SOC) is used to represent the energy status of the OESS during the operation. There are $N+1$ SOC_i during the journey with N Δd_i. SOC for OESS when the train passes Δd_i, denoted as SOC_{i+1}, can be expressed in (17).

$$SOC_{i+1} = SOC_1 + \frac{-\sum_1^i E_{i,dch} + \sum_1^i E_{i,ch} + \sum_1^i \tilde{E}_{i,ch,reg}}{E_{cap}} \tag{16}$$

where SOC_1 is the initial stored energy in OESS, $\tilde{E}_{i,ch,reg}$ is the expected regenerative braking energy charged to the OESS from other trains, and E_{cap} is the capacity of the OESS.

The SOC of OESS needs to be higher than 0 and lower than 1; thus, constraint (17) needs to be added to the model.

$$0 \le SOC_i \le 1 \tag{17}$$

According to the law of conservation of the energy, the conversion of the energy can be expressed in (18).

$$E^+_{i,m} + E^-_{i,m} - E_{i,v} - E_{i,f} - E_{i,p} = 0 \tag{18}$$

As the motor has its traction/braking characteristics, in each Δd_i, the maximum force the motor can conduct should follow the limitation of its maximum traction force $\overline{F_t}$ and maximum braking force $\overline{F_b}$. Also, it needs to be limited by the maximum traction power $\overline{P_t}$ and maximum braking power $\overline{P_b}$. Thus, these can be expressed as shown in (19) and (20).

$$0 \le E^+_{i,m} \le \overline{F_t}\Delta d_i, \quad 0 \le E^-_{i,m} \le \overline{F_b}\Delta d_i \tag{19}$$

$$0 \le E^+_{i,m} \le \overline{P_t}\Delta t_i, \quad 0 \le E^-_{i,m} \le \overline{P_b}\Delta t_i \tag{20}$$

For OESS, the discharged and charged energy cannot exceed the maximum value determined by the maximum charge and discharge power P_o, as expressed in (21).

$$0 \le E_{i,dch} \le \overline{P_o}\Delta t_i, \quad 0 \le E_{i,ch} + \tilde{E}_{i,ch,reg} \le \overline{P_o}\Delta t_i \tag{21}$$

Here $\tilde{P}'_{i,reg,\rho}$ is used to represent the maximum expected regenerative braking power that can be used by the train in each Δd_i in specific power supply section ρ. In this case, the expected regenerative braking energy utilized by the studied train operation in each Δd_i depends on the product of $\tilde{P}'_{i,reg,\rho}$ and Δt_i which is expressed by (22).

$$0 \le \tilde{E}_{i,reg} + \tilde{E}_{i,ch,reg} \le \tilde{P}'_{i,reg,\rho}\Delta t_i \tag{22}$$

D. Linearization of the Model with Integer Variables

The above section proposes a model for EETC with OESS, considering the expected regenerative braking energy utilization. Nevertheless, there are still some equations that need to be linearized by using the integer variables to make the logical section during the operation.

1) Logic of the energy transmission: During the journey, the train cannot conduct traction and braking at the same time; the traction energy in (14) and regenerative energy in (15) of the train cannot exist simultaneously in one Δd_i. Similarly, OESS cannot discharge or be charged simultaneously. Still, the OESS can receive the regenerative braking energy in the environment whenever the train is running on the track, just as shown in Figure 19. In this case, the 0-1 variables $\lambda_{i,1}$, $\lambda_{i,2}$, $\lambda_{i,3}$ and a large number L need to be imposed into the model to determine the train and OESS operation mode in each Δd_i, as shown in (23) - (27).

$$0 \le E_{i,s} \le \lambda_{i,1}L, \quad 0 \le \tilde{E}_{i,reg} \le \lambda_{i,1}L \tag{23}$$

$$0 \le E_{i,ch} \le (1-\lambda_{i,1})L \tag{24}$$

$$0 \le \tilde{E}_{i,ch,reg} \le (1-\lambda_{i,2})L \tag{25}$$

TABLE I
THE VALUE SELECTION OF THE 0-1 VARIABLES $\lambda_{i,1}$, $\lambda_{i,2}$ AND $\lambda_{i,3}$ AND THE RESULTED IN TRAIN OPERATION MODE WITH CORRESPONDING ENERGY FLOW ILLUSTRATION

Value selection	Operation mode	Energy flow illustration
$\lambda_{i,1}$=1, $\lambda_{i,2}$=1, $\lambda_{i,3}$=1.	Motoring	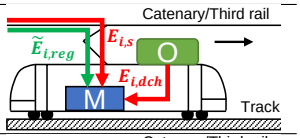
$\lambda_{i,1}$=1, $\lambda_{i,2}$=0, $\lambda_{i,3}$=0.	Motoring	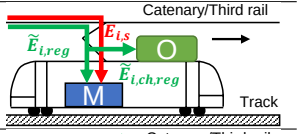
$\lambda_{i,1}$=0, $\lambda_{i,2}$=1, $\lambda_{i,3}$=0.	Braking	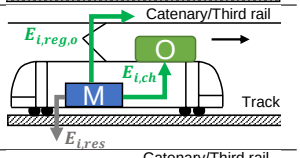
$\lambda_{i,1}$=0, $\lambda_{i,2}$=0, $\lambda_{i,3}$=0.	Braking	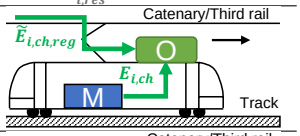
$\lambda_{i,1}$=1, $\lambda_{i,2}$=0, or $\lambda_{i,3}$=0. / $\lambda_{i,1}$=0, $\lambda_{i,2}$=0, $\lambda_{i,3}$=0.	Coasting	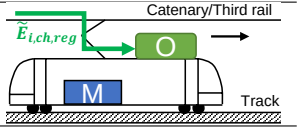

* In all of the figures in the table, the green boxes with "O" inside represent OESSs, and the blue boxes with "M" inside represent motors. The red arrow represents the traction energy from the substation or OESS, the green arrow represents the regenerative braking energy, and the gray arrow represents the energy dissipated by resistors. The black arrow is the running direction.

$$0 \le E_{i,dch} \le \lambda_{i,3} L \tag{26}$$

$$\lambda_{i,3} \le \lambda_{i,1}, \quad \lambda_{i,3} \le \lambda_{i,2}, \quad \lambda_{i,3} \ge \lambda_{i,1} + \lambda_{i,2} - 1 \tag{27}$$

To make it more clear, the value selection of these three 0-1 variables and the resulting train operation mode with different power flows have been shown in Table I. It can be seen that when $\lambda_{i,1}$=1, the traction substation, OESS, and regenerative braking energy in the environment can be transmitted to the train jointly. At the same time, if $\lambda_{i,2}$=1, then $\lambda_{i,3}$=1, the train is motoring, and the discharge process of the OESS can occur; if $\lambda_{i,2}$=0, then $\lambda_{i,3}$ =0, discharge process of OESS does not happen. It represents two possible scenarios: (1) the train is motoring, and the regenerative braking energy in the environment can be charged into the OESS during the traction; (2) the train is coasting, and the regenerative braking energy in the environment can be charged into the OESS when energy from substation and environment to the motor are both assigned to be 0. Contrarily, when $\lambda_{i,1}$=0, then $\lambda_{i,3}$ is always 0, ensuring that the discharging process would not happen simultaneously. The train motor is enabled to regenerate the energy, and the OESS can receive the energy from the motor and environment. At this time, if $\lambda_{i,2}$=1, the train is braking, and the OESS can only be charged by the regenerative braking energy from the train's motor; if $\lambda_{i,2}$=0, it represents two possible scenarios: (1) the train is braking, and the OESS can be charged by the regenerative braking energy from the train's own motor and the environment together; (2) the train is coasting and the regenerative braking energy in the environment can be charged into the OESS when energy from train's own motor is assigned to be 0.

It should be noted that the option that the energy charged to the OESS directly from the substation is naturally avoided since it is an inefficient use of the electricity due to the transmission loss of the grid, the conversion loss of the motor, and the discharging/charging loss of the OESS in the transmission process.

2) Expected regenerative braking power utilization: In (8) and (9), the time-variant expected available regenerative braking power in the environment is approximated by using piecewise linearization, and the time instant for the train's moving by using the middle point of the Δt_i is also shown. To achieve the utilization of the power in the network, the relationship between the time-variant expected available regenerative braking power and time instant need to be established.

To build the relationship between $\tilde{P}'_{i,reg,\rho}$ and time instant t'_i in the model, the integer logical variables α_x, and the auxiliary variables $t'_{i,x}$ are introduced to reformulate the original functions as shown in (28) - (31).

$$\tilde{P}'_{i,reg,\rho} = \sum_{x}^{x+k} a_x t'_{i,x} + b_x \alpha_x \tag{28}$$

$$\alpha_x t_x \le t'_{i,x} \le \alpha_{x+1} t_{x+1}, , \quad \text{for} \quad x = x, x+1, ..., x+k \tag{29}$$

$$\sum_{x}^{x+k} \alpha_x = 1 \tag{30}$$

$$t'_i = \sum_{x}^{x+k} t'_{i,x}, \quad \text{for} \quad i = 1, 2, ..., N \tag{31}$$

In each Δd_i, the corresponding t'_i will be automatically allocated to a specific piecewise linear section.

In (22), the product of the power and time can be linearized by conducting the method in [40]. The auxiliary variables $y_{i,1}$ and $y_{i,2}$ are introduced, as shown in (32).

$$y_{i,1} = \frac{1}{2}(\tilde{P}'_{i,reg,\rho} + \Delta t_i), \quad y_{i,2} = \frac{1}{2}(\tilde{P}'_{i,reg,\rho} - \Delta t_i) \tag{32}$$

In this case, it has the relationships represented by (33).

$$\tilde{P}'_{i,reg,\rho} \Delta t_i = y_{i,1}^2 - y_{i,2}^2 \tag{33}$$

Here one preset series of piecewise points Y_j is used to represent $y_{i,1}$ and $y_{i,2}$. In this case, (33) can be reformulated into (34).

$$\tilde{P}'_{i,reg,\rho} \Delta t_i = \sum_{j=1}^{J} Y_j^2 \alpha_{i,j} - \sum_{j=1}^{J} Y_j^2 \beta_{i,j} \tag{34}$$

where $\alpha_{i,j}$ and $\beta_{i,j}$ are two sets of SOS2 variables for each type of OESS in Δd_i, and J is the number of the corresponding

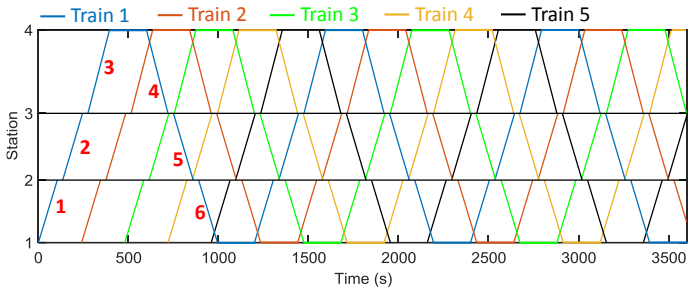

Fig. 5. The first-hour scheduled timetable of the metro system used in the numerical experiment. There are 4 stations with 6 inter-station operations (red solid lines).

piecewise points. As a result, they also need to follow the (35) and (36).

$$\sum_{j=1}^{J} \alpha_{i,j} = 1, \quad \sum_{j=1}^{J} \beta_{i,j} = 1 \tag{35}$$

$$0 \leq \alpha_{i,j} \leq 1, \quad 0 \leq \beta_{i,j} \leq 1 \tag{36}$$

To ensure that only the adjacent $\alpha_{i,j}$ and $\beta_{i,j}$ can be nonzero and their sum is 1, 0-1 variables $\mu^{\alpha}_{i,j}$ and $\mu^{\beta}_{i,j}$ need to be imposed, as shown in (37) - (38).

$$\alpha_{i,j} + \alpha_{i,j+1} - \mu^{\alpha}_{i,j} \geq 0, \quad \beta_{i,j} + \beta_{i,j+1} - \mu^{\beta}_{i,j} \geq 0 \tag{37}$$

$$\sum_{j=1}^{J-1} \mu^{\alpha}_{i,j} = 1, \quad \sum_{j=1}^{J-1} \mu^{\beta}_{i,j} = 1 \tag{38}$$

E. Objective of the Proposed Model

The optimization objective of the proposed model is to minimize the net energy consumption of the train operation from the energy sources, substation, OESS, and environment. The net energy consumption can be expressed by the difference between the traction energy consumption and the recovered energy by OESS, which can be formulated as (39).

$$\min \quad \sum_{i=1}^{N} (\underbrace{E_{i,s} + E_{i,dch} + \tilde{E}_{i,reg}}_{\text{Energy consumed for traction}} \underbrace{- E_{i,ch} - \tilde{E}_{i,ch,reg}}_{\text{Energy recovered by OESS}}) \tag{39}$$

By conducting the optimization, it can be seen that the traction energy consumption, $E_{i,s} + E_{i,dch} + \tilde{E}_{i,reg}$, can be minimized with the support of the energy from OESS and expected utilization of regenerative braking energy, and the expected recovered energy $E_{i,ch}$ and $\tilde{E}_{i,ch,reg}$ by OESS can be maximized.

III. Numerical Experiments

The above sections propose detailed simulation methods for obtaining the expected available regenerative braking power within the railway traction power network. A MILP model for train operation optimization is then developed. In this section, the effectiveness of the proposed optimization framework is verified with numerical experiments.

TABLE II
The Parameters for the Studied Route

Inter-station section	Track length (m)	Scheduled running time (s)	W_S	Q	(μ_s, σ_s^2)
1	1500	105	270	365	$(105, 4.4^2)$
2	1600	110	270	365	$(110, 4.4^2)$
3	2000	120	270	365	$(120, 4.4^2)$
4	2000	120	270	365	$(120, 4.4^2)$
5	1600	110	270	365	$(110, 4.4^2)$
6	1500	105	270	365	$(105, 4.4^2)$

A. Parameters Set-Up

A typical railway traction power network with 4 stations supplied by one traction substation is used in the numerical experiment. Since there are 4 stations in the studied railway system, the number of inter-station train operations is 6, including the up-directional and down-directional ones, as shown in Figure 5 with its first hour's timetable. The scheduled headway is set to be 240 s for each run; thus, there are 15 runs for each inter-station per hour since its first train service. The track length and scheduled running time for each inter-station operation are listed in Table II. Assuming 18 hours of operation for a day q, the total number of the operations W_S is $15 \times 18 = 270$. The running time variation for each inter-station operation is assumed to obey the normal distribution $Nor(\mu_s, \sigma_s^2)$ [41], [42], and the mean value μ_s and the variance σ_s^2 of each inter-station operation are also preset in Table II. μ_s is assumed to be the scheduled running time of each inter-station operation, and σ_s^2 is assumed to make most of the running time variation range from -10 s to 10 s.

The train and OESS parameters used in simulation and optimization are tabulated in Table III. The size of the OESS follows the similar value used in [20], [21], [43]. Noted that the Li-ion battery, flywheel, or any other type of energy storage system can also be used in the proposed method to conduct the optimization, and in this case study, the supercapacitor is used solely due to its more common use as OESS in existing railway lines. Additionally, though the proposed model is flexible enough to take into consideration the varied slope and speed limit of the journey, the track of this numerical experiment is set to be flat. There is no speed limit for all of the inter-station sections in order to avoid the interference of other factors and highlight the direct influence of the energy interaction among train, OESS and regenerative braking energy in the environment on train trajectory changes in the later sections.

It should be noted that the energy transmission efficiency from the traction substation to the motor is set as 90% due to a 10% average energy loss, and the energy conversion efficiency of an electric motor is set as 90% for most typical engineering applications [1]. Therefore, the approximated value for η_s is 81% = 90% $\times$ 90% in this study. On the other hand, energy can be directly transmitted between the motor and OESS with a negligible transmission loss [44]. Thus, the value for η_o is set as 90% considering only the discharge/charge efficiency resulted from the OESS's internal resistance. From [45] and [46], the efficiency for the utilization of the regenerative braking energy from other trains ranges from 0.65 for inter-city railway

TABLE III
THE PARAMETERS FOR THE ROLLING STOCK AND THE OESS USED IN THE NUMERICAL EXPERIMENT

Parameter	Value/Type
Train mass (t)	176
Max traction/braking force (kN)	310
Max traction/braking power (kW)	4000
A (kN)	2.0895
B (kN $\cdot$s/m)	0.0098
C (kN $\cdot$s^2/m^2)	0.0065
Max acceleration/deceleration (m/s^2)	1.2
η_s	0.81
η_o	0.90
η_r	0.85
OESS type	Maxwell® 125V HEAVY TRANSPORTATION MODULE
OESS max power (kW)	1034
OESS mass (t)	0.61
OESS capacity (kWh)	1.4

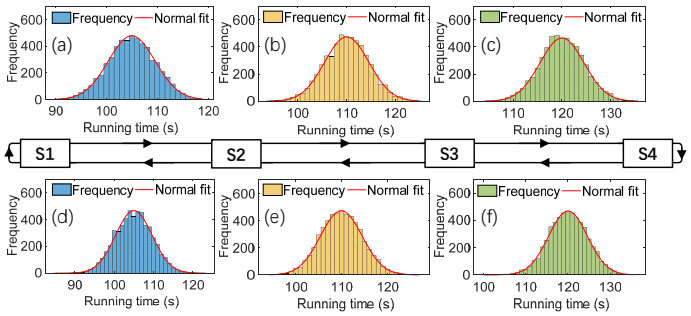

Fig. 6. The sampled running times for inter-station sections 1-6 of the first hour of the studied metro system, where (a) is the sampling histogram for inter-station section 1, (b) for inter-station section 2, (c) for inter-station section 3, (d) for inter-station section 6, (e) for inter-station section 5 and (f) for inter-station section 4.

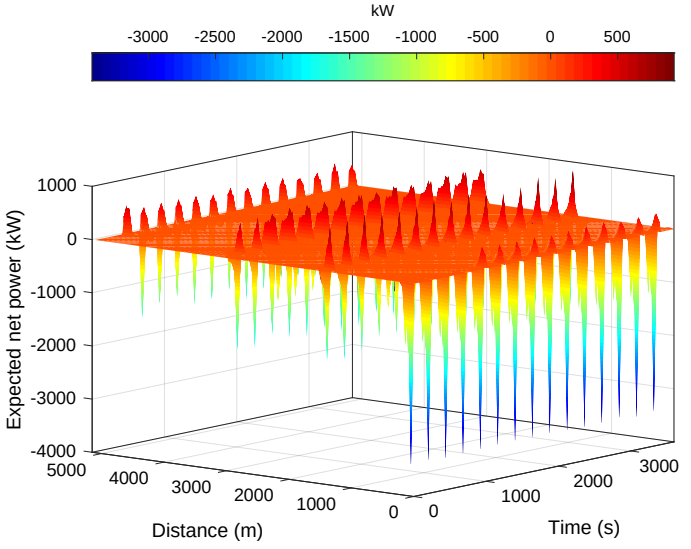

Fig. 7. The heat map of the expected net power for the first hour in the studied metro system after the Monte-Carlo simulation. The sparks in the figure, including positive and negative ones, represent the expected net power that accumulated due to departure or arrival following the stochastic timetable.

systems and 0.95 for urban rail transit systems, here η_r in this paper is set as 85%. In the case study, the power supply system

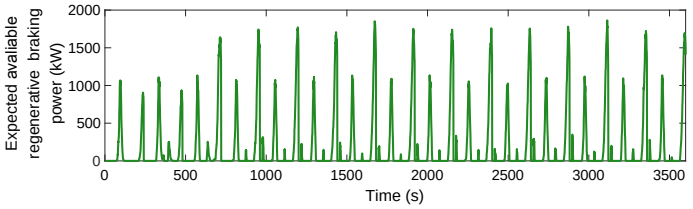

Fig. 8. The expected available regenerative braking power distribution in the first hour of the studied metro system based on the results of the Monte-Carlo simulation. A similar pattern can be found when the train services become stable.

for the studied railway line follows the structure in Figure 2, where the regenerative braking energy will be transmitted via the catenary/third rail and common buses in traction substations, and the corresponding energy transmission efficiency among trains are set to be an average value η_r. However, it should be noted that the proposed method can also be utilized in other types of energy transmission systems by modifying this efficiency value. For instance, if the studied system is the tie feeding system with interconnections between two tracks, the corresponding η_r needs to be changed accordingly (which might be higher than the efficiency of using common buses in traction substation since the transmission distance is shorter). If this value is misused, the expected available regenerative braking energy will see a large error, leading to unpractical results. All in all, these three efficiency values can be modified according to the field data collected from different types of power supply systems, rolling stocks, and different types of OESS.

Note that this experiment is conducted by using Matlab R2020a® and Gurobi® 9.0.1 solver on a PC with Intel Core® i5-6500 processor (3.20 GHz) and 8.00 GB RAM.

B. Monte-Carlo Simulation of the Regenerative Braking Power

As shown in Figure 6, the running time distribution for all the inter-station sections is generated based on the information listed in Table II and Table III. Since Q is set to be 365 to represent the 365 days in one year, the total running time generated for each inter-station operation is $15 \times 365 = 5475$. Due to the difference in the service cycle for each train, some of the inter-station sections see less than 15 operations in the first hour since the first train departs from the initial station, e.g., inter-station section 3 with 14 operations, inter-station section 4 with 13 operations, inter-station section 5 with 12 operations and inter-station section 6 with 12 operations, which is usual in daily operations and does not influence the results of the proposed method.

Due to the fluctuation of the running time of each inter-station operation, the practical timetable for any day in a year is different. This leads to the number of scenarios being 365 and the same probability for each scenario being 1/365=0.0027. Based on the simulation results, the heat map for the expected net power of the studied railway network about the distance and time is shown in Figure 7, and the whole simulation process consumes 315 s in total. It can be seen from the figure that the value of the net power is different at different positions

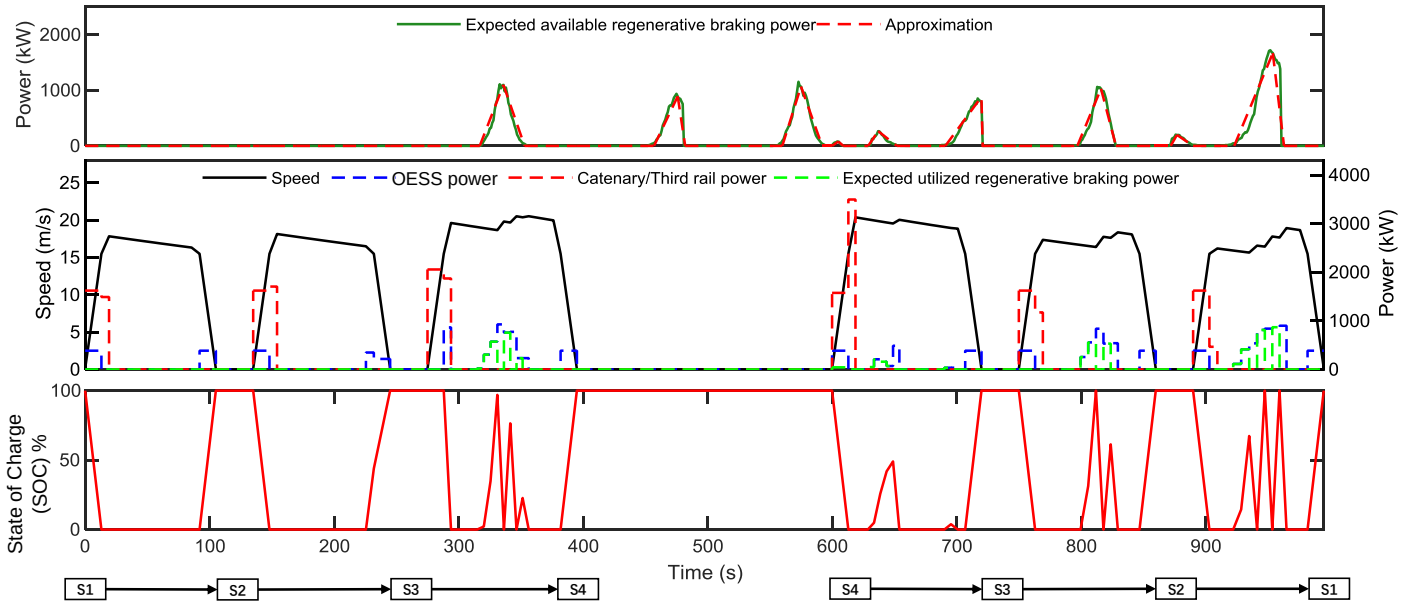

Fig. 9. The optimal train trajectory, catenary/third rail power, OESS power (positive for both discharging and charging, SOC dropping for discharging, and SOC rising for charging) and expected utilized regenerative braking power from other trains for the 1^{st} service cycle of Train 1.

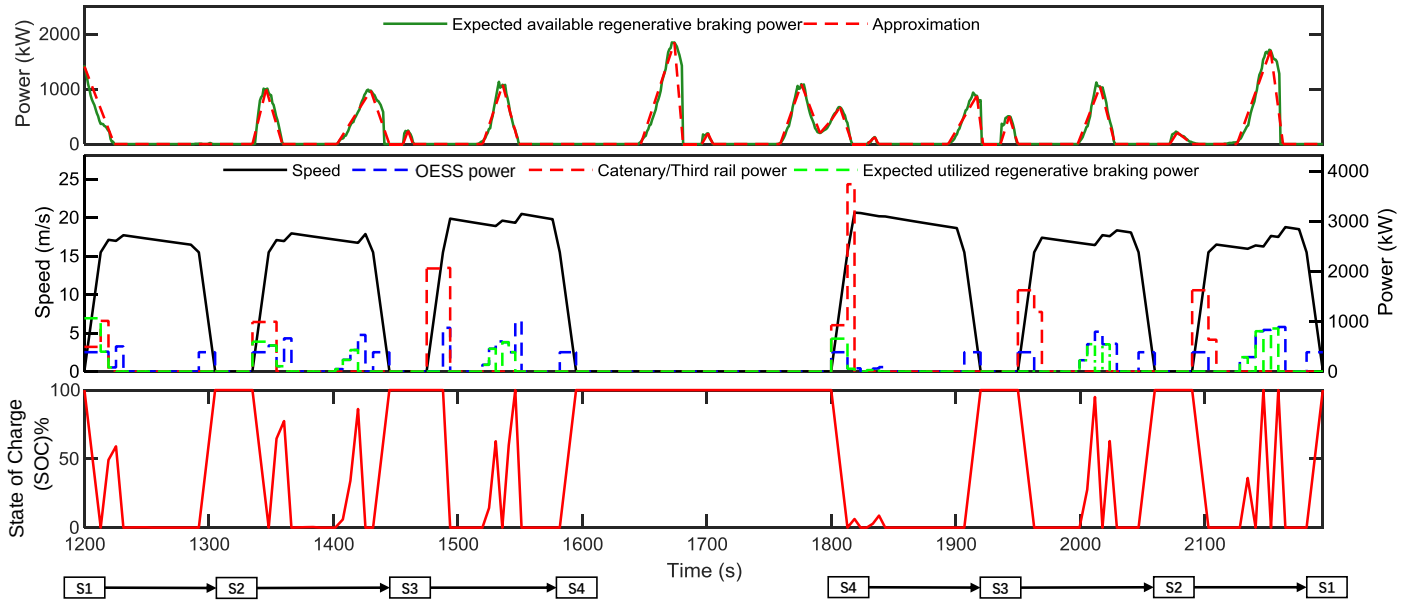

Fig. 10. The optimal train trajectory, catenary/third rail power, OESS power (positive for both discharging and charging, SOC dropping for discharging, and SOC rising for charging) and expected utilized regenerative braking power from other trains for the 2^{nd} service cycle of Train 1.

and time instants. The heat map looks like a timetable since only when the train is braking can the regenerative braking power be generated, and this happens typically near the arrival station. The more trains braking simultaneously, the higher the regenerative braking power in this power supply section will be at that moment. Figure 8 shows the time-variant expected available regenerative braking power in the environment. Though the practical timetable is stochastic and fluctuates, it can be seen that the expected available regenerative braking power in the first hour's operation follows similar patterns with respect to the time when the train service cycles are stable.

C. Train Trajectory Optimization

After obtaining the expected available regenerative braking power in the environment, each of the specific inter-station operations can be optimized using the proposed MILP model. The service cycles for Train 1 (see Figure 5) in the first hour from the initial station to the terminal station are selected to show the optimization results. The running time for each inter-station is fixed to be scheduled running time, as shown in Table II. The time complexity for obtaining the globally optimal result of each service cycle depends on the sum of the computational time of each inter-station section. For the 1^{st} service cycle, its

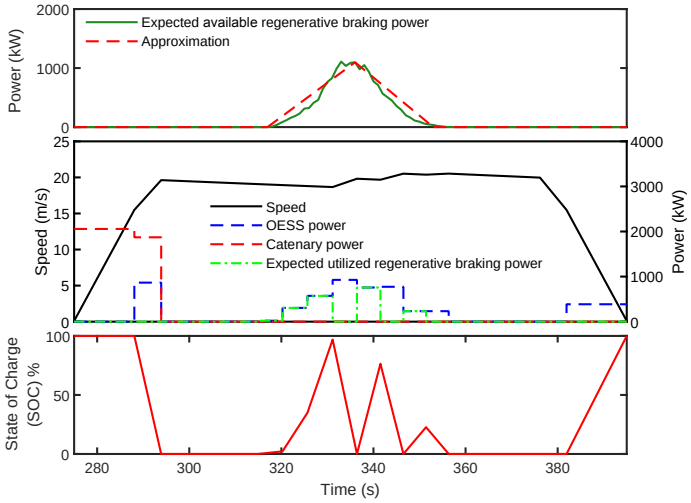

Fig. 11. The optimal train trajectory, catenary/third rail power, OESS power (positive for both discharging and charging, SOC dropping for discharging, and SOC rising for charging), and expected utilized regenerative braking power from other trains for the inter-station operation 3 of the 1^{st} service cycle of Train 1.

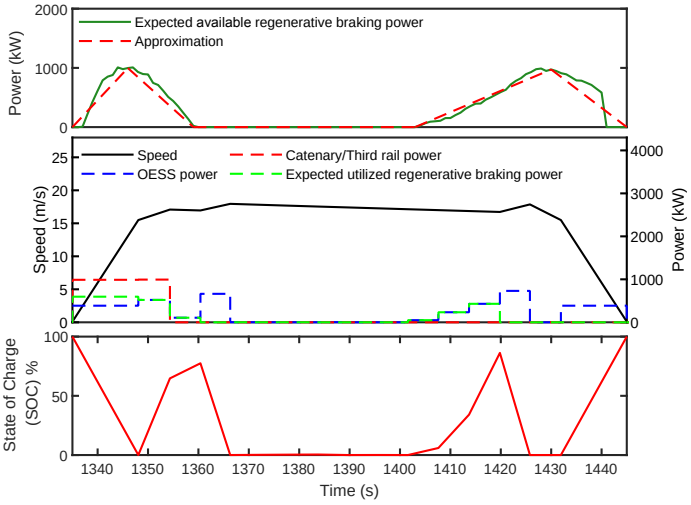

Fig. 12. The optimal train trajectory, catenary/third rail power, OESS power (positive for both discharging and charging, SOC dropping for discharging, and SOC rising for charging), and expected utilized regenerative braking power from other trains for the inter-station operation 2 of the 2^{nd} service cycle of Train 1.

time complexity is 514.90 s in total (0.52 s, 0.43 s, 100.32 s, 122.54 s, 90.65 s, and 200.44 s for inter-station section 1, 2, 3, 4, 5 and 6 respectively). For the 2^{nd} service cycle, it is 736.42 s in total (30.75 s, 140.46 s, 133.21 s, 130.89 s, 80.90 s, and 220.21 s for inter-station sections 1, 2, 3, 4, 5 and 6 respectively). It can be noted that the first two inter-sections for 1^{st} service cycle see the shortest computational time since, at the beginning of the daily operation, there is no available regenerative braking power in the environment that can be utilized; thus no integer variables introduced to build the piecewise sections during the optimization process.

The results are illustrated in Figure 9 and Figure 10, which show the approximation of the expected available regenerative braking power in the environment, optimal train trajectories,

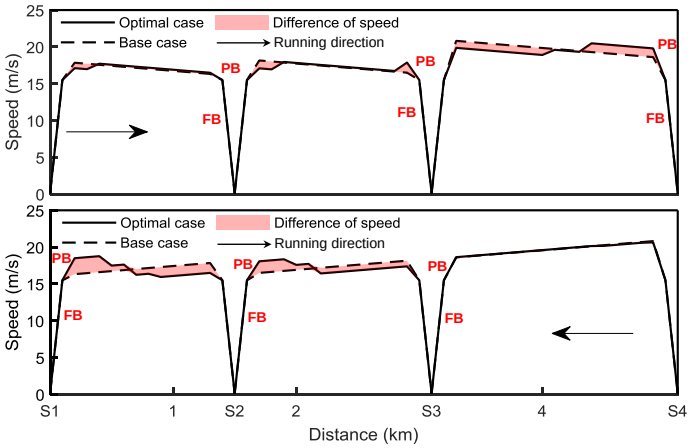

Fig. 13. The comparison between the optimal trajectory resulting from the proposed method (Optimal case) and the base trajectory from the case without the utilization of regenerative braking energy of other trains (Base case).

power profiles, and OESS discharge/charge profiles for the 1^{st} and 2^{nd} service cycles of Train 1. The figures show that the energy from the traction substation, OESS, and regenerative braking energy from other trains are all utilized during one service cycle, shown as the red, blue, and green dashed lines. The train trajectories for all of the inter-station operations are obtained, and the OESS discharge/charge power profiles also change frequently and notably, which shows the OESS releases or receives energy from the studied train and the other trains. Since the track is flat and there is no speed limit, the optimal train trajectory between two adjacent stations in both directions (inter-station sections 1 and 6, 2 and 5, and 3 and 4) should be the same. However, due to the influence of the regenerative braking energy in the environment (power network), the train trajectory for each inter-station section changes accordingly to adjust the train operation status, which results in different adaptive train trajectories. For instance, the train trajectory for the inter-station section 1 is less fluctuated than that for the inter-station section 6 since the regenerative braking energy from other trains in the environment is less. Similar observations can also be found when comparing the train trajectories for inter-station section 2 and 5 and 3 and 4. On the other hand, when comparing the running in the same inter-station section at different times, the influence of the regenerative braking power in the environment on the optimal train operation, referring to the optimal trajectories for inter-station sections 1, 2, and 4 in two service cycles in both Figure 9 and Figure 10.

To demonstrate the energy interaction among the trains, OESS, and the available regenerative braking energy in the environment, the optimal solutions for inter-station operation 3 in Figure 9 and the inter-station operation 2 in Figure 10 are zoomed in here as examples for a more detailed discussion.

Figure 11 presents the optimal solution of the inter-station section 3 of the 1^{st} service cycle of Train 1, and it can be seen that the train firstly uses the energy from the traction substation and the energy stored in the OESS to support its motoring at the beginning of the journey. After the motoring, the train begins to coast, and during the coasting, the regenerative braking energy

from other trains is charged into the OESS, which raises its SOC to nearly 100%. Then, the train begins to re-motor and only uses the energy from OESS. The OESS's process of receiving the regenerative braking energy from the environment and releasing the energy occurs back and forth during the journey, showing the effectiveness of the proposed method on utilization of the available regenerative braking energy by adjusting both the train and OESS operations accordingly. It can also be observed that the OESS power equals the expected regenerative braking power when charging, and it rises first as the expected regenerative braking power increases.

Figure 12 presents the optimal solution of the inter-station section 2 of the 2^{nd} service cycle of Train 1. Due to the occurrence of the regenerative braking energy from other trains at the beginning of the journey, the studied train utilizes the energy from the traction substation, OESS, and other trains together in its traction process. During the motoring mode of the train (from 1335 s to 1366 s), the available regenerative braking energy in the environment can be used to charge the OESS and replace part of the energy from the traction substation during motoring. It is observed that during the later period of the motoring, regenerative braking energy becomes the primary power source of the train. The expected utilized regenerative braking power changes with the power variation trend in the power network environment. This indicates the proposed method can use the energy from other trains as much as possible.

Figure 13 compares the difference between the optimal train trajectory with OESS, taking into account the expected available regenerative braking energy in the environment (Optimal case) and optimal train trajectory with OESS but without regenerative braking energy in the environment (Base case). It can be found the train trajectories for both situations are significantly different. For the base case, fewer fluctuation of the trajectory is found, and more coasting is preferred to save energy consumption. For the optimal case obtained in this paper, slight acceleration for lower speed at the beginning and re-motoring process in the middle of the journey happen frequently. The motoring phase is observed to be postponed to the later operation stages to adapt to the expected time of regenerative braking energy from other trains and utilize more of it. It also should be noted that the optimal results impose an insignificant impact on the obtained expected regenerative braking energy as the same full braking operation ("FB" in Figure 13) occurs only at the end of each inter-station section, which keeps the same trend with the base case before some slightly different or even similar partial braking operation ("PB" in Figure 13) compared with the base case. This indicates that the amount of regenerative braking energy newly added to the environment is insignificant for train-optimized operations based on the proposed method.

D. Energy-Saving Performance

Following the optimization method mentioned in the above sections, the optimal train control strategies for one hour can be obtained, the performance of which is demonstrated by using

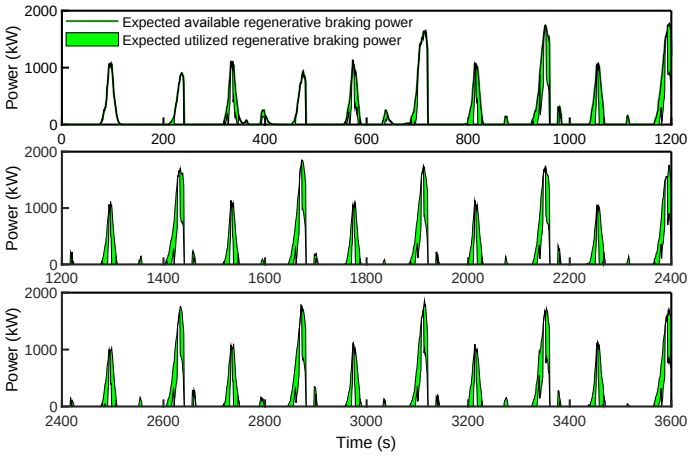

Fig. 14. The expected utilization of the available regenerative braking power in the environment for the studied metro system after the application of the proposed method in the first hour.

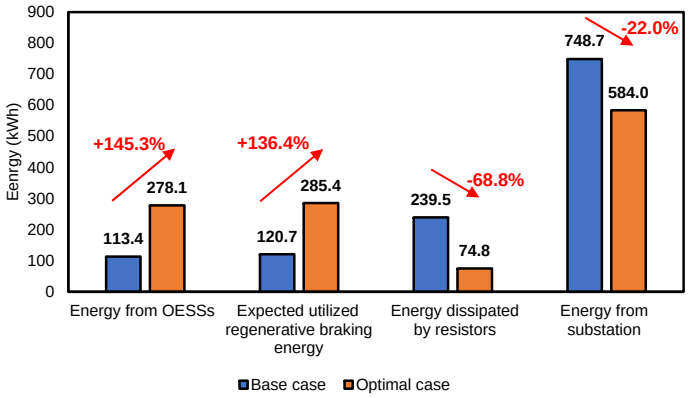

Fig. 15. The energy consumption comparison between the base and optimal cases in one hour. The energy from the traction substation is expected to be significantly reduced by 22%.

the expected utilized regenerative braking power in Figure 14. The figure presents the expected utilized regenerative braking power in one hour. It can be found that most of the time, the regenerative braking energy in the environment is expected to be fully utilized, and 68.8% of available regenerative braking energy is expected to be utilized by using the OESS and adjusting the train trajectory following the optimal solution.

To further show the effectiveness of the proposed method, four indicators are presented here to compare the performance brought by the proposed method (optimal case) and the solution without considering the regenerative braking energy utilization (base case). The four indicators from (40) to (43) are R_{dch}, the expected improvement/reduction rate of the energy from OESSs, R_{reg}, the utilized regenerative braking energy, R_{res}, the energy dissipated by resistors, and R_s, the energy from substation.

$$R_{dch} = (E^O_{dch} - E^B_{dch})/E^B_{dch} \times 100\% \tag{40}$$

$$R_{reg} = (E^O_{reg} - E^B_{reg})/E^B_{reg} \times 100\% \tag{41}$$

$$R_{res} = (E^O_{res} - E^B_{res})/E^B_{res} \times 100\% \tag{42}$$

$$R_s = (E^O_s - E^B_s)/E^B_s \times 100\% \tag{43}$$

where E^O_{dch} and E^B_{dch} are the energy from OESSs of all the train services of optimal case and base case respectively, E^O_{reg} and E^B_{reg} are the utilized regenerative braking energy of all the train services of optimal case and base case respectively, E^O_{res} and E^B_{res} are the energy dissipated by resistors of all the train services of optimal case and base case respectively and E^O_s and E^B_s are the energy from substation of all the train services of the optimal case and base case respectively.

The comparison is illustrated in Figure 15. It can be seen that the energy released by the OESS during each journey of the optimal case reaches 278.1 kWh, which is 145.3% of that of the base case (113.4 kWh). The reason for this large discrepancy is that for the base case, without consideration of the regenerative braking energy utilization, the OESS is normally used at the beginning and the end of the journey without the discharge/charge processes back and forth, like the optimal case in the middle of the journey. When the OESS can receive energy from the environment, it can support the train repeatedly, making the most of the OESS and available regenerative braking energy together. As a result, it can be seen that the regenerative braking energy utilization rate is expected to see a 136.4% increase compared with the base case, and the energy dissipated by resistors is expected to drop by 68.8%. The energy from the traction substation is expected to see a 22.0% reduction, showing the energy-saving potential of the proposed approach.

E. Sensitivity Analysis

The sensitivity analysis of the optimal train trajectory is conducted in this section to validate the effectiveness and robustness of the proposed method. The study adopts two extreme timetable scenarios from the simulation results to show the possible range of energy-saving performance in different train paths.

The first scenario is referred to as the “Min” scenario, representing that all the train services follow the shortest running time in Figure 6 for each inter-station section. Therefore, the running time for inter-station sections 1, 2, 3, 4, 5, and 6 is 90 s, 94 s, 104 s, 100 s, 94 s, and 85 s, respectively. The second scenario is referred to as the “Max” scenario, representing that all the train services follow the longest running time in Figure 6 for each inter-station section. Therefore, the running time for inter-station sections 1, 2, 3, 4, 5, and 6 is 119 s, 125 s, 135 s, 136 s, 127 s, and 123 s, respectively. The selection of these two scenarios is because they both are extreme situations that cause the most significant discrepancies in the train paths compared to the scheduled timetable. This leads to the worst cases in which the available regenerative braking energy distribution is significantly different in the network and hard to coordinate.

The results for utilizing the regenerative braking energy for two worst cases are presented in Figure 16 and Figure 17. It can be observed that the green areas are reduced significantly when compared with Figure 15, showing the lower frequency of the coordination among different trains. Additionally, Figure 18 illustrates the detailed energy-saving performance, i.e., R_{dch}, R_{reg}, R_{res} and R_s, of implementing the proposed optimal trajectory in different train paths. ”Normal” here represents the

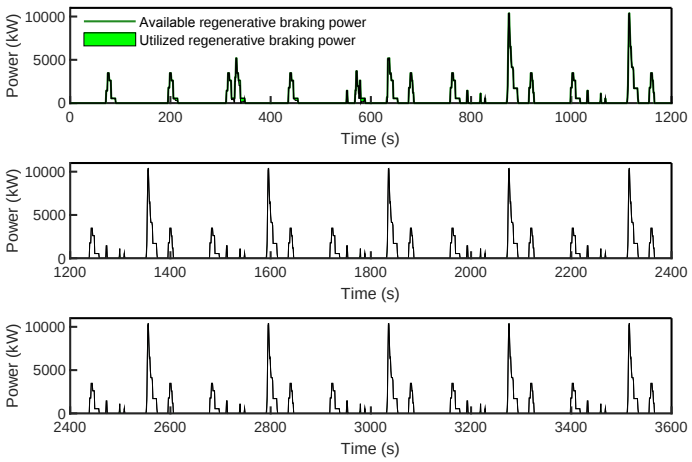

Fig. 16. The utilization of the available regenerative braking power in the environment for the studied metro system for the worst scenario ”Min” in the first hour.

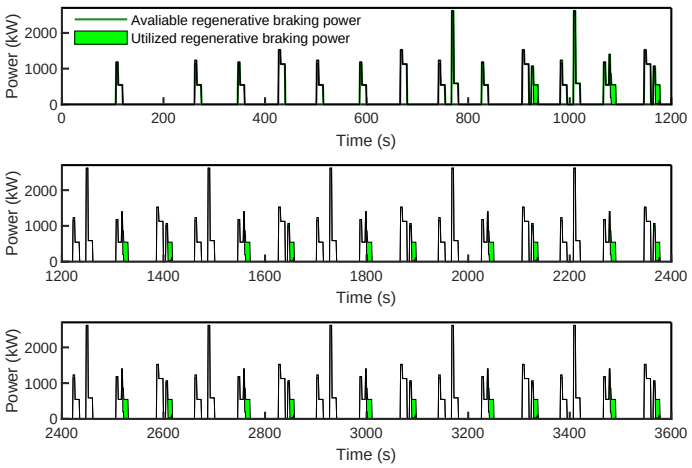

Fig. 17. The utilization of the available regenerative braking power in the environment for the studied metro system for the worst scenario ”Max” in the first hour.

scenario in all of the train services following the simulated distribution (Figure 6) with the results from Figure 15. It can be easily observed that the energy from OESSs and expected utilized regenerative braking energy for the “Min” scenario and ”Max” scenario are much less than the ”Normal” scenario, forming a trend of rising first followed by dropping. Though it is much lower than the ”Normal” scenario, which is more than 130%, it can still see more than 10% and a more than 30% energy-saving improvement compared to the operation without the optimal trajectory. As for the energy dissipated by resistors, the reduction rates for both the “Min” scenario and the “Max” scenario are -3.1% and -14.8%, relatively lower than the ”Normal” scenario.

Similarly, the energy from the substation follows the same trend, such that the value for the ”Min” scenario and ”Max” scenario is much lower than the ”Normal” scenario. A “Normal” scenario can represent the minor-delayed scenario since some inter-station sections have been randomly allocated with the minor-delayed/advanced running time in the sampling process.

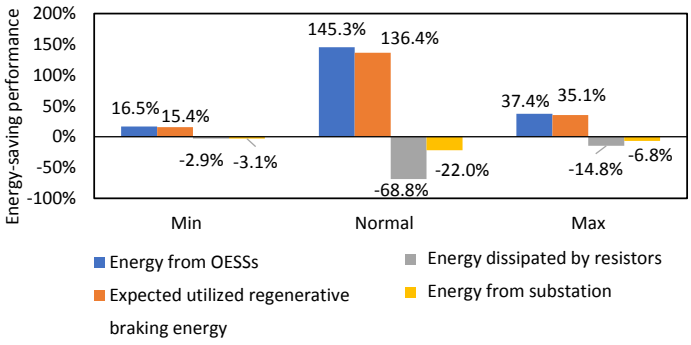

Fig. 18. The energy-saving performance comparison of the three scenarios.

All in all, the energy-saving performance comparison for the worst case and the optimal case is conducted, and it is found that though the energy-saving performance is significantly reduced, the proposed optimal solution can still help cut energy consumption in all aspects.

IV. Conclusion and Future Work

By adopting an agent-environment model, this paper proposes a new approach to optimize the train trajectory with an onboard energy storage system (OESS), considering the utilization of the regenerative braking energy in the environment of the railway power network. Different from most previous studies to simultaneously optimizing the operation of all trains in the network, this paper considers the stochastic available regenerative braking energy as the environment information to be fed into a smart decision-making process using mixed integer linear programming (MILP) for each single-train operation. The expected time-variant available regenerative braking power in the environment can be obtained by employing the Monte-Carlo simulation based on the field data of the stochastic timetable. Then, by integrating the energy support from the traction substation, OESS, and regenerative braking energy from other trains, a MILP model is established to obtain the optimal train trajectory to minimize the expected net energy consumption.

A generic railway system with four stations in one power supply section is used in the numerical experiment in the paper, and the results show that the proposed method can give an optimal solution for minimizing the expected net energy consumption by adjusting the train trajectory and the operation of the OESS to make the most of available regenerative braking energy. In this case, from the results, it can be seen that for a specific service cycle, the energy consumption from the traction substation is expected to be reduced by 22.0%, and 68.8% of regenerative braking energy in the environment is expected to be further utilized for one hour's operation by applying the optimal solution. Also, the energy-saving performance of the worst cases is explored, showing the robustness and usefulness of the proposed method. Since the proposed method can locate the optimal train speed, the solution can be provided directly to train drivers or embedded in a driver advisory system (DAS) and automatic train operation (ATO) system to implement in train operations.

In the future, realistic metro systems can be studied using the method if the field data of stochastic timetables is available. Moreover, the timetable optimization can also be considered to utilize the regenerative braking energy in the network further by extending the current model. Furthermore, it can also be noticed that some sparks of the power in the network can also be found after the optimization. To deal with this, the model can also be extended or modified to reduce the peak power to ensure a safe operation from the perspective of the grid, which is also an exciting topic in the field. Furthermore, the train platforming and routing problem integrated with the train control and OESS management can also enhance the practicality of the proposed model, and extending the model by involving this problem is inspiring.

Appendix
Stochastic Regenerative Braking Energy in the Environment

In real applications, fluctuations of the train running time of each inter-station section always occur in the daily operations [47]–[50], as shown in Figure 19, and it influences the generation and consumption of the regenerative braking energy. The uncertainty of the running time brings the stochastic characteristic on both the value and distribution of the regenerative braking power in each power supply section and the entire railway power network, which leads to challenging applications of the solution given by the traditional timetable and trajectory optimization methods by using deterministic parameters from static environment information.

In this section, the Monte-Carlo simulation is used first to obtain the expected regenerative braking power distribution. The procedure of the stochastic running time generation, the corresponding power distribution obtainment, and the expected available regenerative braking power in the network are given.

A. Scenario Simulation of Stochastic Running time

For obtaining the expected regenerative braking energy distribution in the environment, the railway traffic scenarios need to be found first. Some existing works have explored the methods to generate railway traffic scenarios. For instance, [51] considers a condensed-traffic approach where the dwell time follows the log-normal distribution and the time shift at the terminal station follows the uniform distribution. The work is extended in [52] where the ATO train speed profile and specific module of the traffic regulation system in real-time are involved.

Unlike these studies, this paper mainly takes the running time variation as the primary consideration in scenario generation, and the detailed procedure is shown as the flowchart in Figure 20. The running time for the particular run w of inter-station section s in one specific day q is denoted as $T_{w,s,q}$. Based on the data collected from the industry, running time between two adjacent stations is stochastic due to the unexpected influence of the status of passengers, operators, or rolling stocks. In many papers related to the performance of the train timetable, most of the theoretical distribution models, such as Normal, Exponential, Weibull, and Log-normal distributions, have been

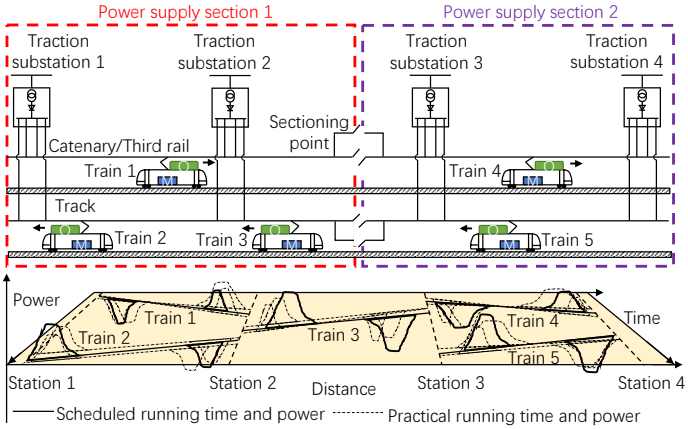

Fig. 19. A schematic illustration of two power supply sections. The power is supplied from adjacent traction substations, with the common buses at substations to transmit the regenerative braking energy, and the difference between the power consumption (negative) and generation (positive) is resulted by scheduled/practical running time. Most power interaction occurs within one section due to the existence of sectioning points (used to separate adjacent power supply sections and are assumed to be kept open in this research), e.g., the regenerative braking energy generated in the power supply section 1 can only be used by the trains running within the same section, i.e., Train 1, Train 2 and Train 3, but not by the trains running in other supply sections, i.e., Train 4 and Train 5 in the power supply section 2 [32], [33], [46].

used to fit statistical models to train running times [48]–[50]. In this case, the running time variation of each inter-station section s is assumed to follow a specific distribution based on the performance analysis of the field running time data. In addition, it is assumed that there are totally S inter-station sections, W_S journeys for each inter-station s, and Q days in the simulation of the studied railway network.

After the running time of all inter-station sections for Q days are obtained, the running time matrix for each day $\boldsymbol{T}^q$ can be constructed. Here the $\boldsymbol{T}^q$ with the same elements are marked as a specific scenario γ with a corresponding number of occurrence day q'_γ. The total number of the scenario is denoted as Γ, then scenario $\boldsymbol{T}^\gamma$ from 1 to Γ can be obtained. In this case, the probability π_γ of each specific scenario γ can be calculated by q'_γ over the total number of days Q, as presented in Figure 20.

B. Expected Regenerative Braking Power

In the above running time simulation by using Monte-Carlo simulation, all scenario $\boldsymbol{T}^\gamma$ and their corresponding probability π_γ from 1 to Γ have been obtained. Then the $\boldsymbol{T}^\gamma$ can be assigned to form the simulated timetable following the base timetable of the studied railway system, as shown in Figure 21-(a). The departure headway for the first train at the initial station and the dwell time at each station are assumed to remain unchanged as the scheduled base value in the simulation process.

After the simulated timetable of all scenarios is made, the power distribution of each scenario can be produced by using the simulation model proposed in [23] based on each $\boldsymbol{T}^\gamma$, as illustrated in Figure 21-(b). The model proposed in [23] can simulate the motoring power outstripping the OESS discharge power and the regenerative braking power outstripping the OESS charge power. Here, the regenerative braking energy is

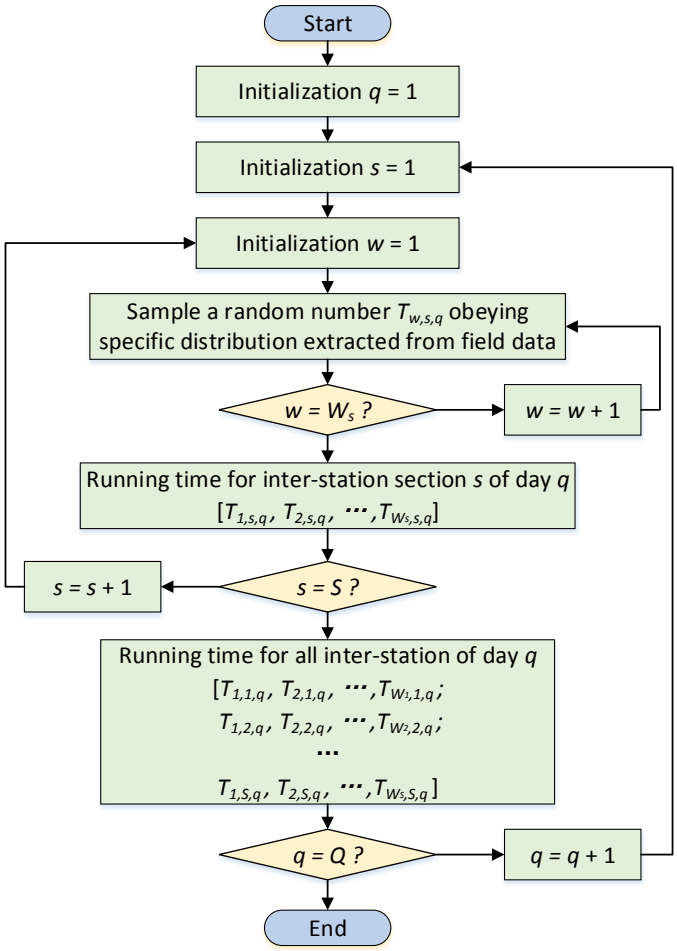

Fig. 20. The flowchart of the Monte-Carlo simulation by sampling the running time for all of the inter-station operations and conducting the statistics analysis of the generated scenarios.

positive, and the motoring power is negative. The energy status, also called the state of charge (SOC) of OESS, for all sampled trains is controlled following the rule that the OESS is fully charged (SOC=100%) before the departure of each train's first service of the day and SOC will not be adjusted at any stations for later operation. Assuming ρ is used to index each power supply section in the studied railway system, as shown in Figure 21-(c), the time-variant net power distribution can be obtained by summing all of the negative and positive power on same time instant in same power supply section since some released regenerative braking energy would be used instantly by the motoring train. By eliminating the negative part of the net power distribution, the rest of the regenerative braking power forms the time-variant available regenerative braking power distribution $P_{reg,\gamma,\rho}$ in the environment for each scenario in each power supply section, as presented in Figure 21-(d). As shown in Figure 21-(e), the next step is to calculate the expected value by multiplying the power distribution of each scenario with its corresponding probability π_γ, then the expected available regenerative braking power for each power supply section $\tilde{P}_{reg,\rho}$ can be simulated and obtained, as presented in Figure 21-(f).

By following the above procedures shown in both Figure 20

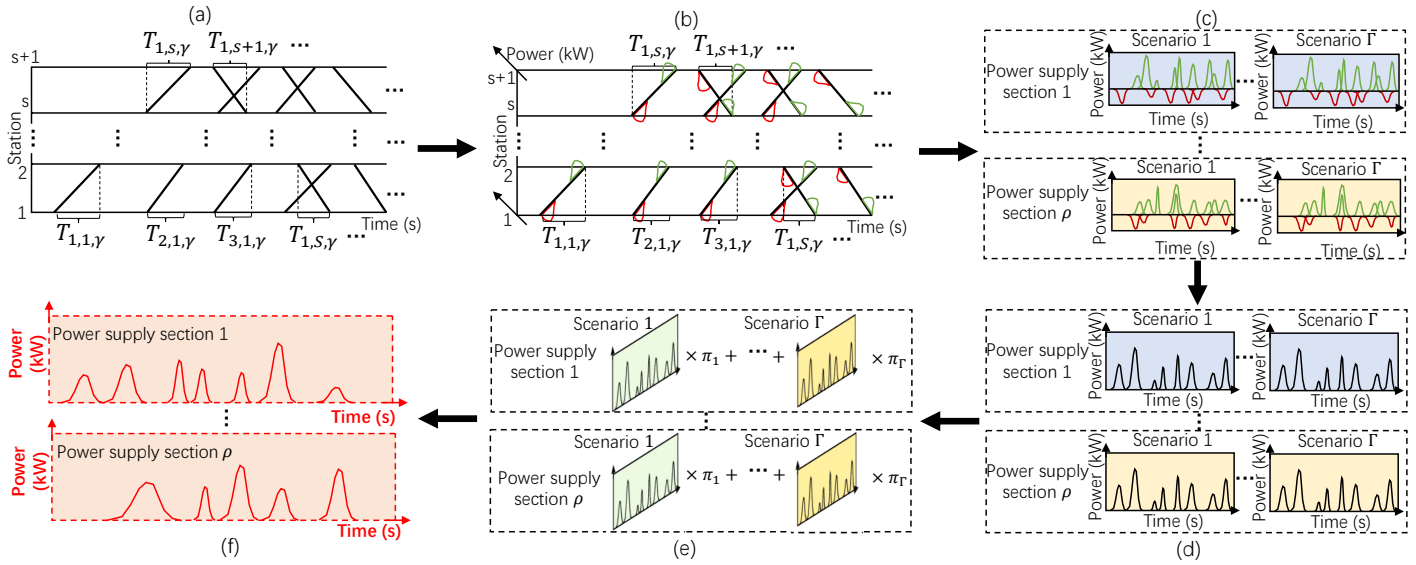

Fig. 21. The procedure to obtain the expected time-variant regenerative braking power distribution of the metro system: (a) Simulate the timetable of each scenario using $\boldsymbol{T}^{\gamma}$ following the base timetable of the studied system; (b) Simulate the power distribution of each scenario of the studied system (The red lines and green lines are the power profiles of the trains: red lines underneath the station-time plane represent the power consumed by trains, and green ones over the station-time plane represent the regenerative braking power); (c) Calculation of the time-variant net power values of all scenarios for all power supply sections; (d) Time-variant available regenerative braking power distribution of all scenarios for all power supply sections; (e) Calculation of the expected value based on all scenarios for all power supply sections; (f) Expected time-variant available regenerative braking power distribution for all power supply sections.

and Figure 21, the statistical parameters of all inter-station sections derived from the historical data can be used and converted to the distribution and expected value of the regenerative braking power of the entire railway network based on the Monte-Carlo simulation.

References

[1] A. González-Gil, R. Palacin, P. Batty, and J. Powell, "A systems approach to reduce urban rail energy consumption," *Energy Conversion and Management*, vol. 80, pp. 509–524, 2014.

[2] Z. Tian, N. Zhao, S. Hillmansen, C. Roberts, T. Dowens, and C. Kerr, "Smartdrive: Traction energy optimization and applications in rail systems," *IEEE Transactions on Intelligent Transportation Systems*, vol. 20, no. 7, pp. 2764–2773, 2019.

[3] M. Saeed, F. Briz, J. M. Guerrero, I. Larrazabal, D. Ortega, V. Lopez, and J. J. Valera, "Onboard Energy Storage Systems for Railway: Present and Trends," *IEEE Open Journal of Industry Applications*, vol. 4, pp. 238–259, 2023.

[4] E. Fedele, D. Iannuzzi, and A. Del Pizzo, "Onboard energy storage in rail transport: Review of real applications and techno-economic assessments," *IET Electrical Systems in Transportation*, vol. 11, no. 4, pp. 279–309, 2021.

[5] B. Zhang, S. Lu, Y. Peng, C. Wu, G. Meng, M. Feng, and B. Liu, "Impact of on-board hybrid energy storage devices on energy-saving operation for electric trains in dc railway systems," *Batteries*, vol. 8, no. 10, p. 167, 2022.

[6] K. Ichikawa, "Application of optimization theory for bounded state variable problems to the operation of train," *Bulletin of JSME*, vol. 11, pp. 857–865, 1968.

[7] P. Howlett, "The optimal control of a train," *Annals of Operations Research*, vol. 98, pp. 65–87, 12 2000.

[8] E. Khmelnitsky, "On an optimal control problem of train operation," *IEEE Transactions on Automatic Control*, vol. 45, pp. 1257–1266, 7 2000. [Online]. Available: http://ieeexplore.ieee.org/document/867018/

[9] R. Liu and I. M. Golovitcher, "Energy-efficient operation of rail vehicles," *Transportation Research Part A: Policy and Practice*, vol. 37, no. 10, pp. 917–932, 2003. [Online]. Available: http://www.sciencedirect.com/science/article/B6VG7-49HMSCM-1/2/39cf1bcd86ae5724b527830488e0e625

[10] A. Albrecht, P. Howlett, P. Pudney, X. Vu, and P. Zhou, "The key principles of optimal train control—part 1: Formulation of the model, strategies of optimal type, evolutionary lines, location of optimal switching points," *Transportation Research Part B: Methodological*, vol. 94, pp. 482–508, 2016. [Online]. Available: http://dx.doi.org/10.1016/j.trb.2015.07.023

[11] ——, "The key principles of optimal train control—Part 2: Existence of an optimal strategy, the local energy minimization principle, uniqueness, computational techniques," *Transportation Research Part B: Methodological*, vol. 94, pp. 509–538, 2016. [Online]. Available: https://www.sciencedirect.com/science/article/pii/S0191261515002076

[12] S. Lu, S. Hillmansen, T. K. Ho, and C. Roberts, "Single-Train Trajectory Optimization," *IEEE Transactions on Intelligent Transportation Systems*, vol. 14, no. 2, pp. 743–750, jun 2013. [Online]. Available: http://ieeexplore.ieee.org/document/6410425/

[13] J. T. Haahr, D. Pisinger, and M. Sabbaghian, "A dynamic programming approach for optimizing train speed profiles with speed restrictions and passage points," *Transportation Research Part B: Methodological*, vol. 99, pp. 167–182, 2017.

[14] P. Wang and R. M. P. Goverde, "Multiple-phase train trajectory optimization with signalling and operational constraints," *Transportation Research Part C: Emerging Technologies*, vol. 69, no. Supplement C, pp. 255–275, 2016. [Online]. Available: http://www.sciencedirect.com/science/article/pii/S0968090X16300766

[15] S. Lu, M. Q. Wang, P. Weston, S. Chen, and J. Yang, "Partial Train Speed Trajectory Optimization Using Mixed-Integer Linear Programming," *IEEE Transactions on Intelligent Transportation Systems*, vol. 17, no. 10, pp. 2911–2920, oct 2016.

[16] Y. Wang, B. De Schutter, T. J. J. van den Boom, and B. Ning, "Optimal trajectory planning for trains – A pseudospectral method and a mixed integer linear programming approach," *Transportation Research Part C: Emerging Technologies*, vol. 29, no. 0, pp. 97–114, 2013. [Online]. Available: http://www.sciencedirect.com/science/article/pii/S0968090X13000193

[17] R. Miao, C. Wu, K. Zhu, F. Xue, Z. Tian, S. Hillmansen, C. Roberts, and S. Lu, "Integrated optimisation model for neutral section location planning and energy-efficient train control in electrified railways," *IET Renewable Power Generation*, vol. 14, no. 18, pp. 3599–3607, 2020.

[18] M. Feng, C. Wu, S. Lu, and Y. Wang, "Notch-based speed trajectory optimisation for high-speed railway automatic train operation," *Proceedings of the Institution of Mechanical Engineers, Part F: Journal of Rail and Rapid Transit*, vol. 236, no. 2, pp. 159–171, 2022.

[19] M. Miyatake and K. Matsuda, "Energy saving speed and charge/discharge

control of a railway vehicle with on-board energy storage by means of an optimization model," *IEEJ Transactions on Electrical and Electronic Engineering*, vol. 4, no. 6, pp. 771–778, 2009.

[20] M. Miyatake and H. Ko, "Optimization of train speed profile for minimum energy consumption," *IEEJ Transactions on Electrical and Electronic Engineering*, vol. 5, no. 3, pp. 263–269, 2010.

[21] Y. Huang, L. Yang, T. Tang, Z. Gao, F. Cao, and K. Li, "Train speed profile optimization with on-board energy storage devices: A dynamic programming based approach," *Computers & Industrial Engineering*, vol. 126, pp. 149 – 164, 2018.

[22] N. Ghaviha, M. Bohlin, and E. Dahlquist, "Speed profile optimization of an electric train with on-board energy storage and continuous tractive effort," in *2016 international symposium on power electronics, electrical drives, automation and motion (speedam)*. IEEE, 2016, pp. 639–644.

[23] C. Wu, W. Zhang, S. Lu, Z. Tan, F. Xue, and J. Yang, "Train speed trajectory optimization with on-board energy storage device," *IEEE Transactions on Intelligent Transportation Systems*, vol. 20, no. 11, pp. 4092–4102, 2019.

[24] C. Wu, S. Lu, F. Xue, L. Jiang, and J. Yang, "Optimization of speed profile and energy interaction at stations for a train vehicle with on-board energy storage device," in *2018 IEEE Intelligent Vehicles Symposium (IV)*, June 2018, pp. 1–6.

[25] C. Wu, B. Xu, S. Lu, F. Xue, L. Jiang, and M. Chen, "Adaptive eco-driving strategy and feasibility analysis for electric trains with on-board energy storage devices," *IEEE Transactions on Transportation Electrification*, 2021.

[26] C. Wu, S. Lu, F. Xue, L. Jiang, M. Chen, and J. Yang, "A two-step method for energy-efficient train operation, timetabling and on-board energy storage device management," *IEEE Transactions on Transportation Electrification*, pp. 1–1, 2021.

[27] X. Wang, P. Sun, Q. Wang, J. Ding, and X. Feng, "Joint optimization combining the capacity of subway on-board energy storage device and timetable," *IET Intelligent Transport Systems*, 2022.

[28] T. Albrecht, "Reducing power peaks and energy consumption in rail transit systems by simultaneous train running time control," *WIT Transactions on The Built Environment*, 2004.

[29] X. Li and H. K. Lo, "An energy-efficient scheduling and speed control approach for metro rail operations," *Transportation Research Part B: Methodological*, vol. 64, pp. 73 – 89, 2014.

[30] ——, "Energy minimization in dynamic train scheduling and control for metro rail operations," *Transportation Research Part B: Methodological*, vol. 70, pp. 269 – 284, 2014.

[31] H. Tang, C. T. Dick, and X. Feng, "Improving regenerative energy receptivity in metro transit systems: Coordinated train control algorithm," *Transportation Research Record Journal of the Transportation Research Board*, vol. 2534, pp. 48–56, 2015.

[32] X. Yang, X. Li, Z. Gao, H. Wang, and T. Tang, "A cooperative scheduling model for timetable optimization in subway systems," *IEEE Transactions on Intelligent Transportation Systems*, vol. 14, no. 1, pp. 438–447, 2012.

[33] X. Yang, A. Chen, X. Li, B. Ning, and T. Tang, "An energy-efficient scheduling approach to improve the utilization of regenerative energy for metro systems," *Transportation Research Part C: Emerging Technologies*, vol. 57, pp. 13–29, 2015.

[34] Z. Tian, P. Weston, N. Zhao, S. Hillmansen, C. Roberts, and L. Chen, "System energy optimisation strategies for metros with regeneration," *Transportation Research Part C: Emerging Technologies*, vol. 75, pp. 120–135, 2017.

[35] X. Sun, H. Lu, and H. Dong, "Energy-efficient train control by multi-train dynamic cooperation," *IEEE Transactions on Intelligent Transportation Systems*, vol. 18, no. 11, pp. 3114–3121, 2017.

[36] S. Su, X. Wang, Y. Cao, and J. Yin, "An energy-efficient train operation approach by integrating the metro timetabling and eco-driving," *IEEE Transactions on Intelligent Transportation Systems*, 2019.

[37] S. Su, X. Wang, T. Tang, G. Wang, and Y. Cao, "Energy-efficient operation by cooperative control among trains: A multi-agent reinforcement learning approach," *Control Engineering Practice*, vol. 116, p. 104901, 2021.

[38] Y. Rao, X. Feng, Q. Wang, P. Sun, Z. Xiao, and H. Chen, "Energy-efficient control of a train considering multi-trains power flow," *IET Intelligent Transport Systems*, vol. 16, no. 3, pp. 380–393, 2022.

[39] Y. Huang, L. Yang, T. Tang, Z. Gao, F. Cao, and K. Li, "Train speed profile optimization with on-board energy storage devices: A dynamic programming based approach," *Computers and Industrial Engineering*, vol. 126, no. January, pp. 149–164, 2018. [Online]. Available: https://doi.org/10.1016/j.cie.2018.09.024

[40] J. Bisschop, "Linear programming tricks," *AIMMS-Optimization Modeling*, pp. 63–75, 2006.

[41] M. Shakibayifar, A. Sheikholeslami, and F. Corman, "A simulation-based optimization approach to reschedule train traffic in uncertain conditions during disruptions," *Scientia Iranica*, vol. 25, no. 2, pp. 646–662, 2018.

[42] E. Hassannayebi, A. Sajedinejad, A. Kardannia, M. Shakibayifar, H. Jafari, and E. Mansouri, "Simulation-optimization framework for train rescheduling in rapid rail transit," *Transportmetrica B: Transport Dynamics*, vol. 9, no. 1, pp. 343–375, 2021.

[43] C. Wu, S. Lu, F. Xue, L. Jiang, and M. Chen, "Optimal sizing of onboard energy storage devices for electrified railway systems," *IEEE Transactions on Transportation Electrification*, vol. 6, no. 3, pp. 1301–1311, 2020.

[44] A. González-Gil, R. Palacin, and P. Batty, "Sustainable urban rail systems: Strategies and technologies for optimal management of regenerative braking energy," *Energy conversion and management*, vol. 75, pp. 374–388, 2013.

[45] G. M. Scheepmaker and R. M. P. Goverde, "Energy-efficient train control including regenerative braking with catenary efficiency," in *2016 IEEE International Conference on Intelligent Rail Transportation (ICIRT)*, 2016, pp. 116–122.

[46] X. Yang, B. Ning, X. Li, and T. Tang, "A two-objective timetable optimization model in subway systems," *IEEE Transactions on Intelligent Transportation Systems*, vol. 15, no. 5, pp. 1913–1921, 2014.

[47] T. Huisman and R. J. Boucherie, "Running times on railway sections with heterogeneous train traffic," *Transportation Research Part B: Methodological*, vol. 35, no. 3, pp. 271–292, 2001.

[48] J. Lessan, L. Fu, C. Wen, P. Huang, and C. Jiang, "Stochastic model of train running time and arrival delay: a case study of wuhan–guangzhou high-speed rail," *Transportation Research Record*, vol. 2672, no. 10, pp. 215–223, 2018.

[49] F. Liu, R. Xu, W. Fan, and Z. Jiang, "Data analytics approach for train timetable performance measures using automatic train supervision data," *IET Intelligent Transport Systems*, vol. 12, no. 7, pp. 568–577, 2018.

[50] P. Kecman and R. M. Goverde, "Predictive modelling of running and dwell times in railway traffic," *Public Transport*, vol. 7, no. 3, pp. 295–319, 2015.

[51] Álvaro J López-López, R. R. Pecharromán, A. Fernández-Cardador, and A. P. Cucala, "Improving the traffic model to be used in the optimisation of mass transit system electrical infrastructure," *Energies*, vol. 10, no. 8, 2017.

[52] D. Roch-Dupré, A. P. Cucala, R. R. Pecharromán, a. J. López-López, and A. Fernández-Cardador, "Evaluation of the impact that the traffic model used in railway electrical simulation has on the assessment of the installation of a reversible substation," *International Journal of Electrical Power & Energy Systems*, vol. 102C, pp. 201–210, 2018.

Chaoxian Wu was born in 1992 in Beihai, Guangxi, China. He received the BEng in Traffic Engineering from Tongji University, Shanghai, China, in 2015. He was awarded his Intercollegiate MSc degree in Transport and Sustainable Development from Imperial College London, UK, and University College London, UK, in 2016. He received his PhD in Electrical Engineering and Electronics from the University of Liverpool, UK, in 2021. He is currently an assistant professor at the School of Systems Science and Engineering, Sun Yat-Sen University, Guangzhou, China. His main research interests are transportation system modelling and operation optimization, energy-saving strategies in transportation systems, smart transportation, and systems theory and science.

Shaofeng Lu received the B.Eng. and Ph.D. degrees from the University of Birmingham, Birmingham, UK, in 2007 and 2011, respectively, and the B.Eng. degree from the Huazhong University of Science and Technology, Wuhan, China, in 2007, all in electrical and electronic engineering.

He is currently a Professor at the Shien-Ming Wu School of Intelligent Engineering, South China University of Technology, Guangzhou, China. His current research interests include optimal operation of railway systems, orderly charging of electric vehicles, optimization of charging facility configuration, etc.

Zhongbei Tian received the B.Eng in Huazhong University of Science and Technology, Wuhan, China, in 2013. He received the B.Eng. and PhD degree in Electrical and Electronic Engineering from the University of Birmingham, Birmingham, U.K., in 2013 and 2017. He is currently an Assistant Professor in Transport Energy Systems at the University of Birmingham. He has been leading a number of projects funded by EPSRC, Royal Society, Horizon 2020, Network Rail, RSSB, and Innovate UK. His research interests include railway traction power system modelling and analysis, energy-efficient train control, energy system optimisation, and sustainable transport energy systems integration and management.

Fei Xue was born in 1977 in Tonghua of Jilin province in China. He received the bachelor and master degrees in power system and its automation from Wuhan University, Wuhan, China, in 1999 and 2002, respectively, and the Ph.D. degree in electrical engineering from Politecnico di Torino, Torino, Italy, 2009. He was the Deputy Chief Engineer of Beijing XJ Electric Company, Ltd and Lead Research Scientist in Siemens Eco-City Innovation Technologies (Tianjin) Company, Ltd. He is currently a Senior Associate Professor and Head of the Department of Electrical and Electronic Engineering, Xi'an Jiaotong-Liverpool University, Suzhou, China. His research interest include power system security, virtual microgrids, electric vehicle, and transactive energy control.

Lin Jiang (Member, IEEE) received the B.Sc. and M.Sc. degrees from the Huazhong University of Science and Technology, Wuhan, China, and the Ph.D. degree from the University of Liverpool, Liverpool, U.K., in 1992, 1996, and 2001, respectively, all in electrical engineering. He is currently a Reader with the Department of Electrical Engineering and Electronics, University of Liverpool, U.K. His research interests include control and analysis of smart grid, renewable energy and power electronics.